**Porphyrins**
**Пофирины**

Макрогетероциклы
http://macroheterocycles.isuct.ru

**Review**
**Обзор**

# Advances in the Synthesis of Porphyrin−Fullerenes

Viktoriya S. Lebedeva,[a@] Nadezhda A. Mironova,[a] Ramzes D. Ruziev,[b]
and Andrey F. Mironov[a]

[a]*MIREA-Russian Technological University, 119454 Moscow, Russian Federation*
[b]*Scientific Centre for Expert Evaluation of Medicinal Products, 127051 Moscow, Russian Federation*
[@]*Corresponding author E-mail: phsstr@gmail.com*

*The review focuses current research in the synthesis, properties, and potential applications of covalently linked porphyrin- and chlorin-fullerenes. An overview of the most popular methods to prepare porphyrin- and chlorin-$C_{60}$ fullerene conjugates is given.*

**Keywords**: Porphyrins, fullerenes, photoinduced electron transfer, photosensitizers, photodynamic therapy.

# Достижения в синтезе порфирин−фуллеренов

В. С. Лебедева,[a@] Н. А. Миронова,[a] Р. Д. Рузиев,[b] А. Ф. Миронов[a]

[a]*МИРЭА – Российский технологический университет, 119454 Москва, Российская Федерация*
[b]*Научный центр экспертизы средств медицинского применения, 127051 Москва, Российская Федерация*
[@]*E-mail: phsstr@gmail.com*

*Обзор посвящен текущим исследованиям в области синтеза, свойств и потенциальных применений ковалентно связанных порфирин- и хлорин-фуллеренов. Дается обзор наиболее популярных методов получения конъюгатов порфирин- и хлорин-$C_{60}$ фуллерена.*

**Ключевые слова:** Порфирины, фуллерены, фотоиндуцированный перенос электрона, фотосенсибилизаторы, фотодинамическая терапия.

## Introduction

Unique electronic and photophysical features of porphyrins and fullerenes lead to great interest in creation of hybrid structures based on them. Porphyrin macrocycle, its di- and tetrahydro derivatives absorb light at wide range between UV and near IR-region, which allows to use similar compounds as light-absorbing antennas. Porphyrins are the basis of pigments, participating in natural photosynthesis, they being quite stable and being able to undergo various chemical functionalization pathways. They possess small HOMO-LUMO gap, which makes them very redox active, and the introduction of different metals into their macrocycle alters their redox potentials.[1] Fullerenes, in contrast to porphyrins, absorb visible light weakly, they being excellent electron-acceptors. Fullerene $C_{60}$, similarly to quinones, the naturally occurring electron acceptors, is readily reduced to form stable radical pairs when coupled to a donor.[2] Besides, $C_{60}$ has small reorganization energy resulting from its rigid spherical shape and π-system delocalization.[3,4] Under irradiation of porphyrin-fullerene structures after the excitation of porphyrin macrocycle either energy transfer with the fullerene activation either electron transfer to fullerene takes place, the ion-radical pair being formed. The combination of porphyrins and $C_{60}$ in the donor-acceptor systems allows to obtain a long-living charge-separated states as the speed of charge recombination is substantially lower than the speed of charge separation.[5] There have been published a considerable number of papers on molecular photosystems based on porphyrins and fullerenes synthesis (beginning with simple donor-acceptor dyads till multichromophoric systems), as well as on supramolecular structures using different kinds of non-covalent interactions (hydrogen bonds, anion

binding, metal-ligand coordination, crown ether-ammonium cation binding, electrostatic interactions and π-π-stacking) in order to simulate natural photosynthetic systems and to study the basic principles of the photoinduced energy and electron transfer in antenna-reaction centers, as well as with the aim of creation of artificial storage and energy transfer systems.[6-18] For a number of the covalent-bound porphyrin-fullerene systems the charge-separation lifetime was comparable and even exceeded the lifetime of the charge-separated state in the natural bacterial photosynthetic reactive center.

The photodynamic activity of porphyrin- and chlorin-fullerenes is also studied with the aim to create novel efficient photosensitizers for the photodynamic therapy of cancer and antimicrobial photodynamic inactivation. When photoinduced, fullerenes transform into the triplet state almost in 100 % quantum yield and then generate efficiently the singlet oxygen or superoxide anion – radical and other active radicals, giving rise to destruction of tumor cells and microorganisms.[19-22] Thus, the two types of effects during the PDT, in which the acting agents are favorably either superoxide radicals or singlet oxygen for the fullerenes coexist. In this connection they can be more efficient when carrying out the PDT under the cancer hypoxia conditions. Fullerene, however, absorb poorly in the visible and IR regions of spectrum, which are the most convenient for using in PDT. In this connection the combination of fullerene with porphyrins and chlorins, which absorb light intensively in this region and transfer the excitation energy or electron to fullerene allow to solve this problem.

Several methods to prepare covalently linked porphyrin- and chlorin-fullerenes are known.

## 1. The Methods of Porphyrin-Fullerene Conjugates Production

Among the fullerene modification methods known[23-26] for the porphyrin- and chlorin-fullerene synthesis the following methods are used most often: the Bingel reaction, $C_{60}$ condensation with butadienes and the Prato reaction. The first technique is based on the condensation of porphyrins, containing the residue of malonic ester, with $C_{60}$ effected by treatment with iodine in the presence of bases (the Bingel reaction) (Scheme 1).

The second technique is the condensation of porphyrins, containing the butadiene residue, with $C_{60}$: the successive conducting of enyne metathesis and the Diels-Alder reaction. The terminal alkyne interacts with olefin in the presence of the Grubbs catalyst and the substituted butadiene being formed condenses with $C_{60}$ when heated (Scheme 2).

1,3-Dipolar cycloaddition of ylide being formed as a result of condensation of N-methylglycine (sarcosine) with formyl-containing porphyrin to fullerene is the basis of the third method – the Prato reaction (Scheme 3).

The last approach is widely used in the synthesis of porphyrin-fullerenes. The intermediate azomethine ylide being formed in the course of the reaction reacts with the $C_{60}$ double bonds yielding pyrrolidine-fullerene (Scheme 4). The pyrrolidine cycle formed binds between the two 6-membered fullerene cycles.
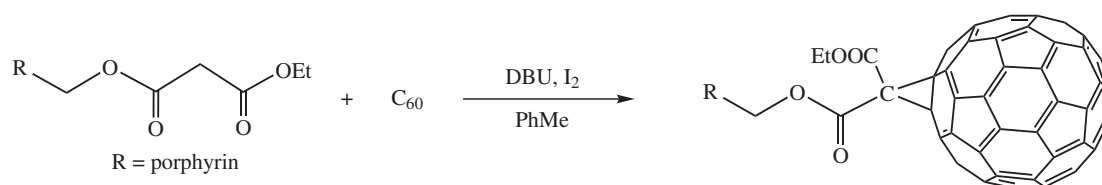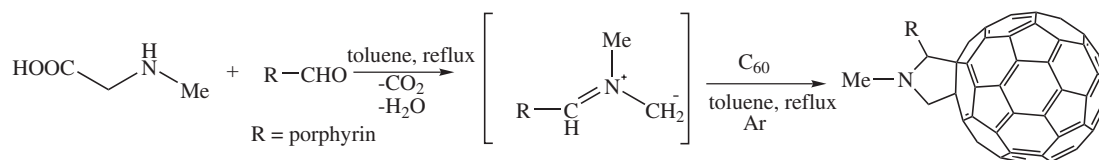


Scheme 1. $C_{60}$ conjugates synthesis using the malonic acid derivatives.
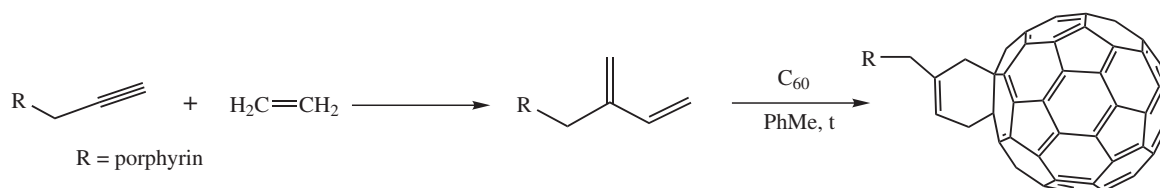


Scheme 2. The condensation of butadiene-substituted porphyrin derivatives with $C_{60}$.
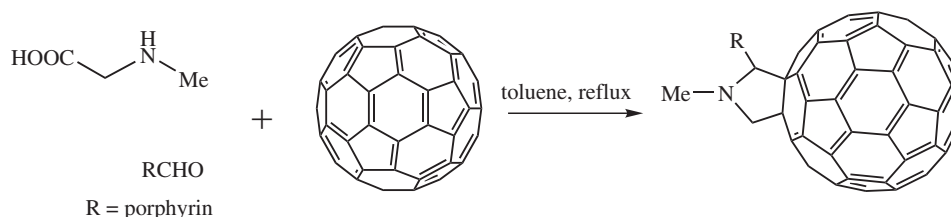


Scheme 3. The Prato method.

**Scheme 4.** The Prato reaction mechanism.

The application of some other *N*-substituted glycines instead of *N*-methylglycine promotes the administration of two different substituents into the pyrrolidine ring.[27-31] Great excess of amino acid and aldehyde may result in the formation of fullerene with 2, 3 and more pyrrolidine moieties.

Lately the substantial modification of the Prato method was proposed, based on cycloaddition of nitryl oxide at the fullerene double bond in the presence of diacetoxyiodobenzene (Scheme 5).[32] The condensation involved in contrast to the Prato reaction proceeds under mild conditions with notably high yields. The isoxazoline cycle produced may possess different substituents at the position 3. Such fullerene derivatives are shown to be efficient electron acceptors.

The arylation of hexa-chlorin substituted fullerene $C_{60}Cl_6$ according Friedel-Crafts by phenylacetic and benzylmalonic acids with the production of $C_{60}(Ar)_5Cl$ is a suitable approach to the production of water-soluble fullerene derivatives (Scheme 6). $C_{60}Cl_6$ is synthesized preliminary by interaction of $C_{60}$ and ICl in 1,2-dichlorbenzene at 40 °C under the pressure ~1 mbar.[33] Complex ethers groups saponification leads to the formation of $C_{60}$ derivatives with 5 and 10 carboxy groups. The condensation
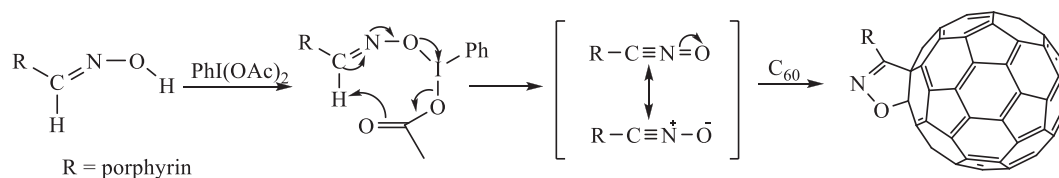


**Scheme 5.** Synthesis of $C_{60}$ conjugates using nitrile oxides.



$R_1 = COOMe, CH(COOMe)_2$
$R_1 = COOH, CH(COOH)_2$
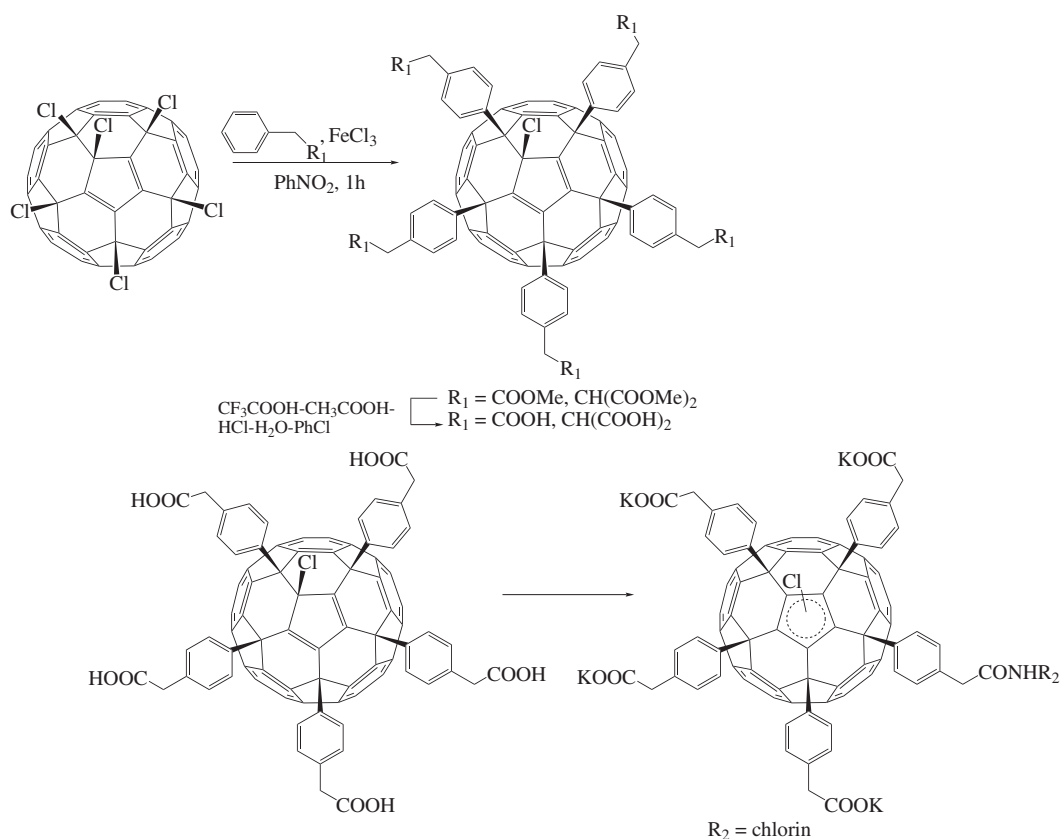
$R_2 = chlorin$

**Scheme 6.** Synthesis of $C_{60}$ derivatives with 5 and 10 carboxy groups and water-soluble chlorin-$C_{60}$.

of chlorins containing amino group with such derivatives promotes the production of conjugates which are highly soluble in water.[34]

## 2. Donor-Acceptor Porphyrin- and Chlorin-Fullerene Systems

Considerable number of various dyads, triads and multi-chromaphoric compounds was synthesized and it was shown that energy or electron transfer occurs in them when photoexcited. The photoinduced electron transfer from the excited singlet state of porphyrin or chlorin donor to fullerene results in the formation of a system with separated charges, its lifetime depending on energy of this state, the type of a linker between the donor and acceptor molecules as well as on the nature of solvent.

Models based on porphyrin- and chlorin-fullerenes are created to study the photosynthesis mechanism and to create artificial solar energy converters.

## 2.1. Dyads of Porphyrins and Chlorins with $C_{60}$ Fullerene

The first porphyrin-fullerene dyad – porphyrin zinc complex – $C_{60}$ **2** described in literature was synthesized by the interaction of diene-substituted porphyrin **1** and $C_{60}$ according to the Diels-Alder reaction (Scheme 7).[35] The time-resolved fluorescence spectroscopy demonstrated that
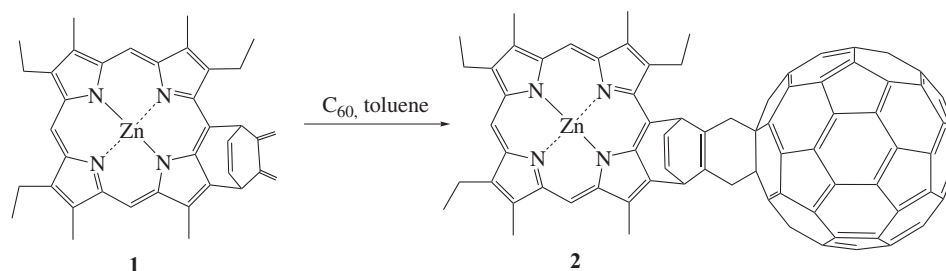


**Scheme 7.** Synthesis of dyad **2** by the Diels-Alder method.
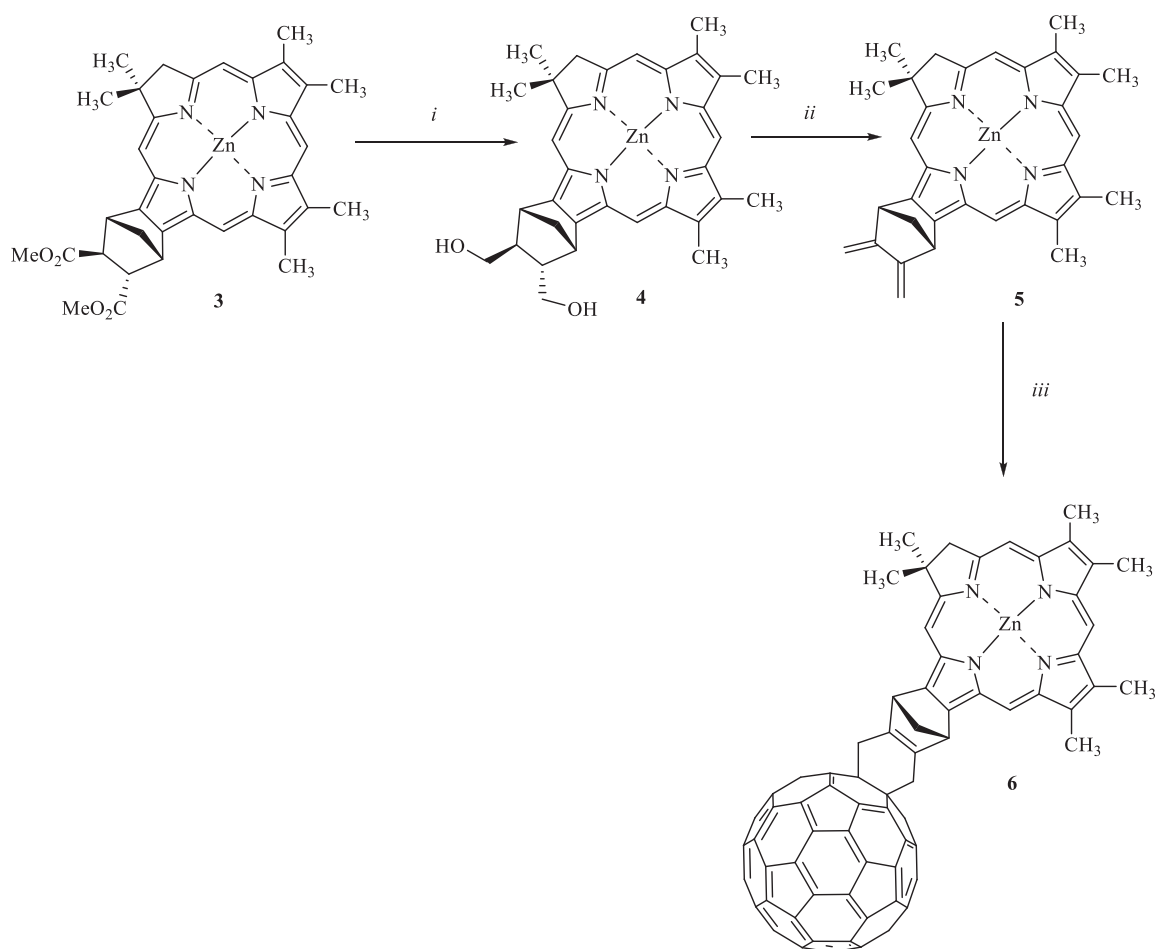


**Scheme 8.** Synthesis of zinc chlorin–$C_{60}$ dyad with a rigid spacer. Reagents and conditions: *i* – LiAlH$_4$, THF, 35 ºC; *ii* – *o*-O$_2$NPhSeCN, nBu$_3$P, 55 ºC (a), H$_2$O$_2$, THF (b); *iii* – C$_{60}$, toluene, reflux..

when the dyad is photoexcited in toluene and benzonitrile the charge-separated state $ZnP^{\bullet+}-C_{60}^{\bullet-}$ is generated as a result of the electron transfer from porphyrin to fullerene with the rate constant $k_{CS}=10^{11}$ s$^{-1}$.

The dyad based on synthetic chlorin and fullerene $C_{60}$ **6** with a rigid spacer was synthesized using the Diels-Alder reaction to minimize electronic interaction between donor and acceptor (Scheme 8).[36] The preformed initial zinc chlorin **3** was turned into diol **4**, and subsequently into diene **5**. Zinc chlorin–$C_{60}$ dyad was synthesized by boiling the latter with $C_{60}$ in toluene for further investigation of the donor-acceptor distance impact to the characteristics of the molecular dyads.

The substituted butadienes were also used in the synthesis of $C_{60}$ conjugate with chlorin $p_6$ cycloimide.[37] The initial purpurin 18 (**7**) reacted with propargylamine in toluene at 80 °C forming ethinylcycloimide **8** with 80 % yield (Scheme 9), its treatment with ethylene in the presence of the Grubbs catalyst affording the compound **9** with 40 % yield. The conjugate **10a** (30 % yield) was obtained by heating diene **9** with $C_{60}$ in toluene. To study the electron transfer, the dyad **10a** was transformed into zinc complex **10b**. The emission intensity of the chlorin component in the fluorescence spectra of the conjugates **10a** and **10b** was noticeably less than that of the initial chlorin, demonstrating an efficient electron transfer towards $C_{60}$.

Fullerene $C_{60}$ nucleophilic cyclopropanation using malonic acid substituted derivatives is one of the widespread approaches to the porphyrin–$C_{60}$ conjugates production.[38-42] The conjugates **11** and **12** were prepared according to this technique (Figure 1).[38,39] Zinc porphyrin in the conjugate **11** is rigidly connected at the two opposite sites with $C_{60}$. In the conjugate **12** porphyrin is attached only at one site of the fullerene.[39] Despite these differences, photophysical and electrochemical features of the compounds **11** and **12** were similar, showing, in the authors' opinion, the significant contribution of non-covalent interactions between zinc porphyrin and fullerene to the general distribution of electron density.

Porphyrin-fullerene dyads with chromophores' location "face-to-face" were synthesized *via* the Bingel reaction of cyclopropanation **13-16** (Figure 2).[43-47] For the compounds **13-16**, as well as in the cases of other dyads, porphyrin's fluorescence in the photoinduced excited state is almost quenching due to the energy or electron transfer from the excited singlet state of porphyrin to fullerene.

Thorough photophysical examinations of the compounds synthesized **13-16** demonstrated that, as contrasted to the other porphyrin–$C_{60}$ dyads generating the charge-separated state only in the polar solvents, $ZnP^{\bullet+}-C_{60}^{\bullet-}$ charge-separated state is produced both in polar and non-polar solvents under photoexcitation of the systems **13-16** the lifetime of the charge-separated state in the polar solvents decreasing significantly.[43-46]

A water-soluble dyad Zn-TPP-$C_{60}$ **17** containing dendron Newkome was synthesized by the authors (Fig-
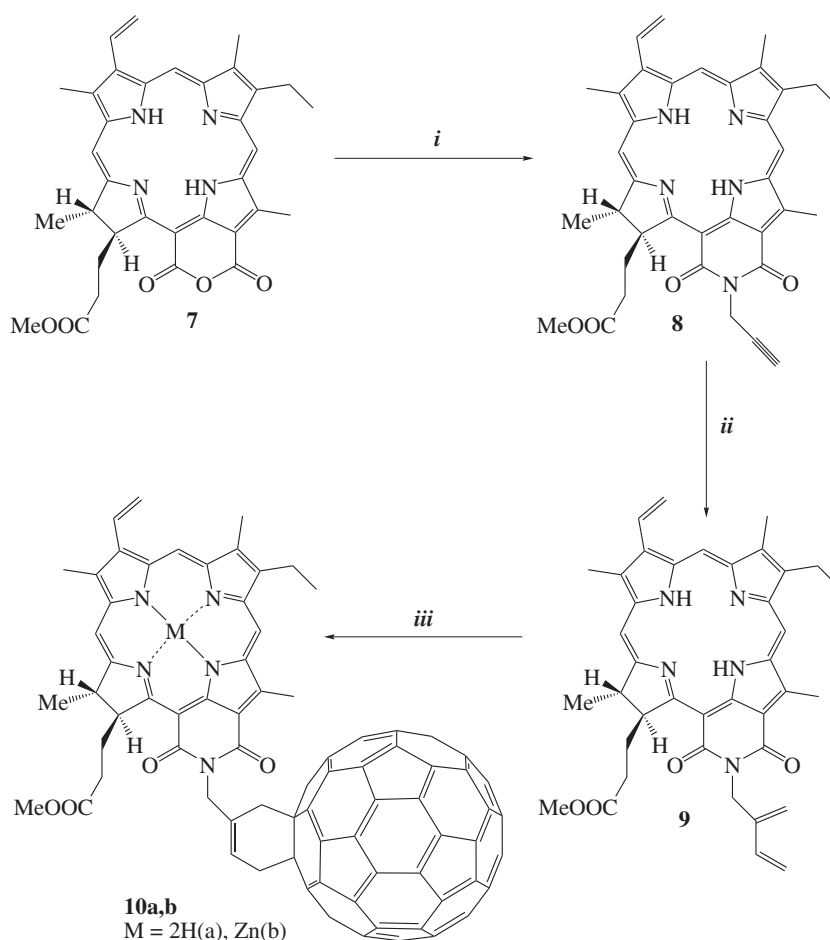


**Scheme 9.** Synthesis of chlorin–$C_{60}$ conjugates **10a,b**. Reagents: *i* - propargylamine; *ii* - $H_2C=CH_2$; *iii* – $C_{60}$ (a), Zn(OAc)$_2$ (b).
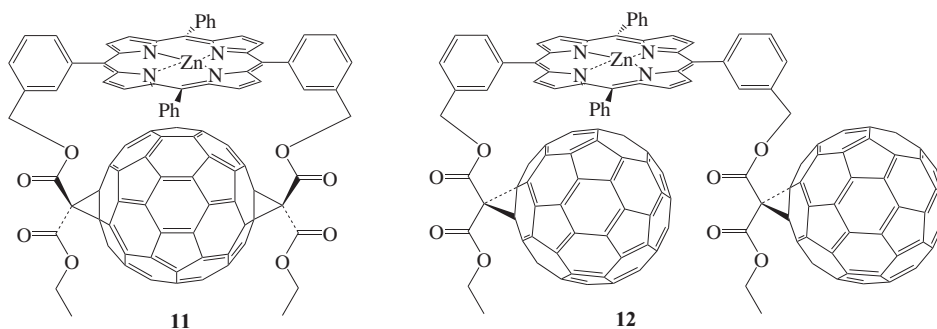
**Figure 1.** Structures of porphyrin-fullerenes with cyclopropane bridges.
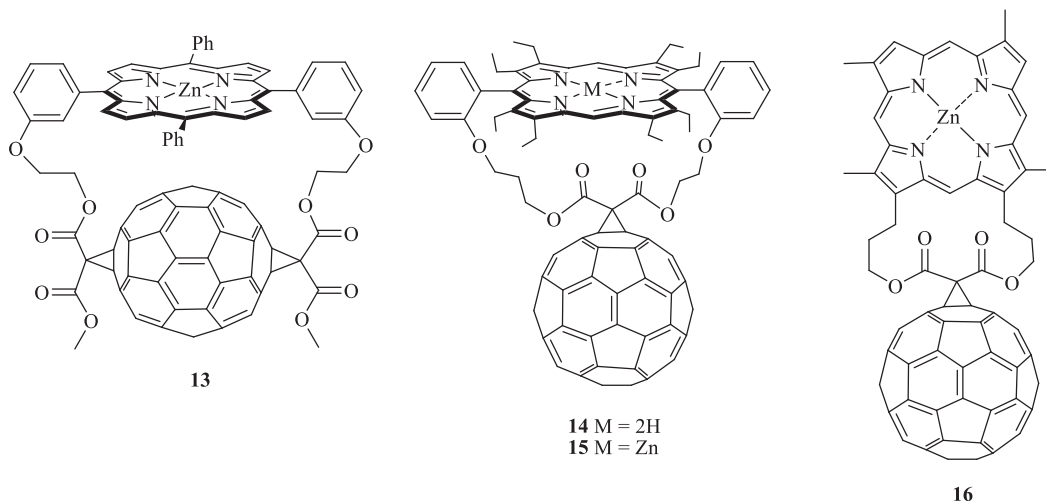


**Figure 2.** Structures of porphyrin–C$_{60}$ dyads with chromophore's location "face-to-face".
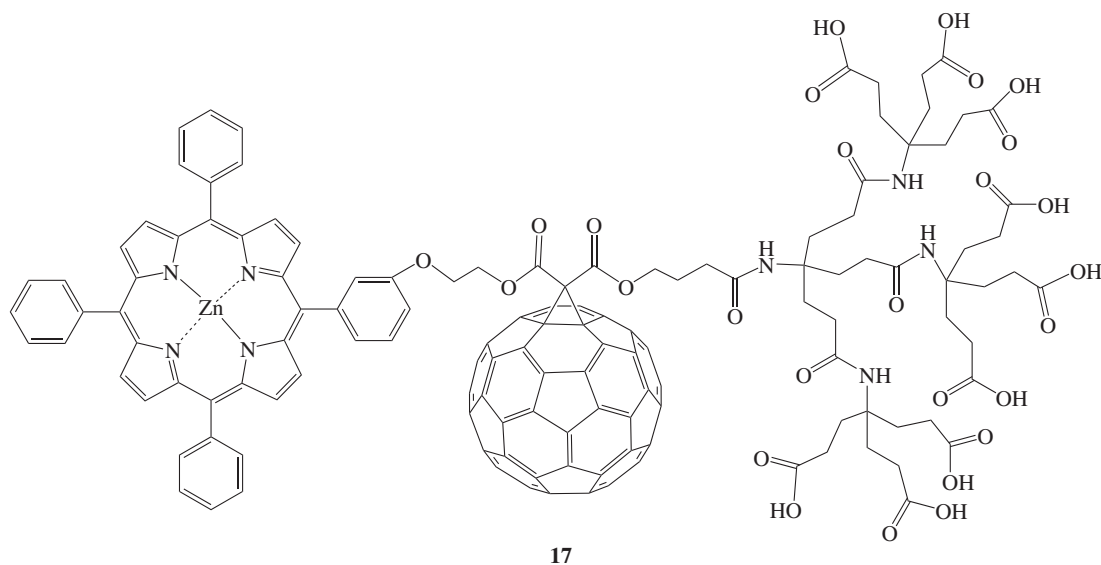


**Figure 3.** Structure of water soluble Zn-TPP-C$_{60}$ dyad.

ure 3).[48] However, the pronounced hydrophilic moiety along with the hydrophobic porphyrin-fullerene segment present in this aggregate resulted in the formation of micellar aggregates in water and precluded the charge distribution studies.

Cyclopropanation using the malonic acid derivatives enabled more complicated adducts of fullerene C$_{60}$ to be obtained.[49] The reaction conditions allowing to synthesize fullerene both with 1 and 6 malonate molecules were worked out. The proposed multi-attachment terms were applied

for hexa-substituted fullerene synthesis with one residue of porphyrin **20a,b** (Scheme 10). The initial porphyrin **18** was condensed with C$_{60}$ *via* the Bingel method and the dyad obtained **19** was treated with ferrocenylmalonate to form hexa-adduct **20a** (30 % yield), which was successively turned to zinc complex **20b**.[49]

The attachment of several malonic ester moieties disturbs significantly the conjugation of π-electronic fullerene system and reduces its electrophilic characteristics, result-ing in the photoinduced transfer lesion. In this connection the bis-pyropheophorbide *a* and fullerene – C$_{60}$ conjugate **21** (Figure 4) obtained by the authors,[50] modified with 5 moieties of malonic ester, can be regarded not as a donor-acceptor system but merely as a carrier for drug delivery.

Using the formyl-substituted *meso*-arylporphyrins presents one of the applications of the Prato reaction for the fullerene-porphyrin conjugate synthesis in which porphyrin and fullerene are bound *via* pyrrole linkers.
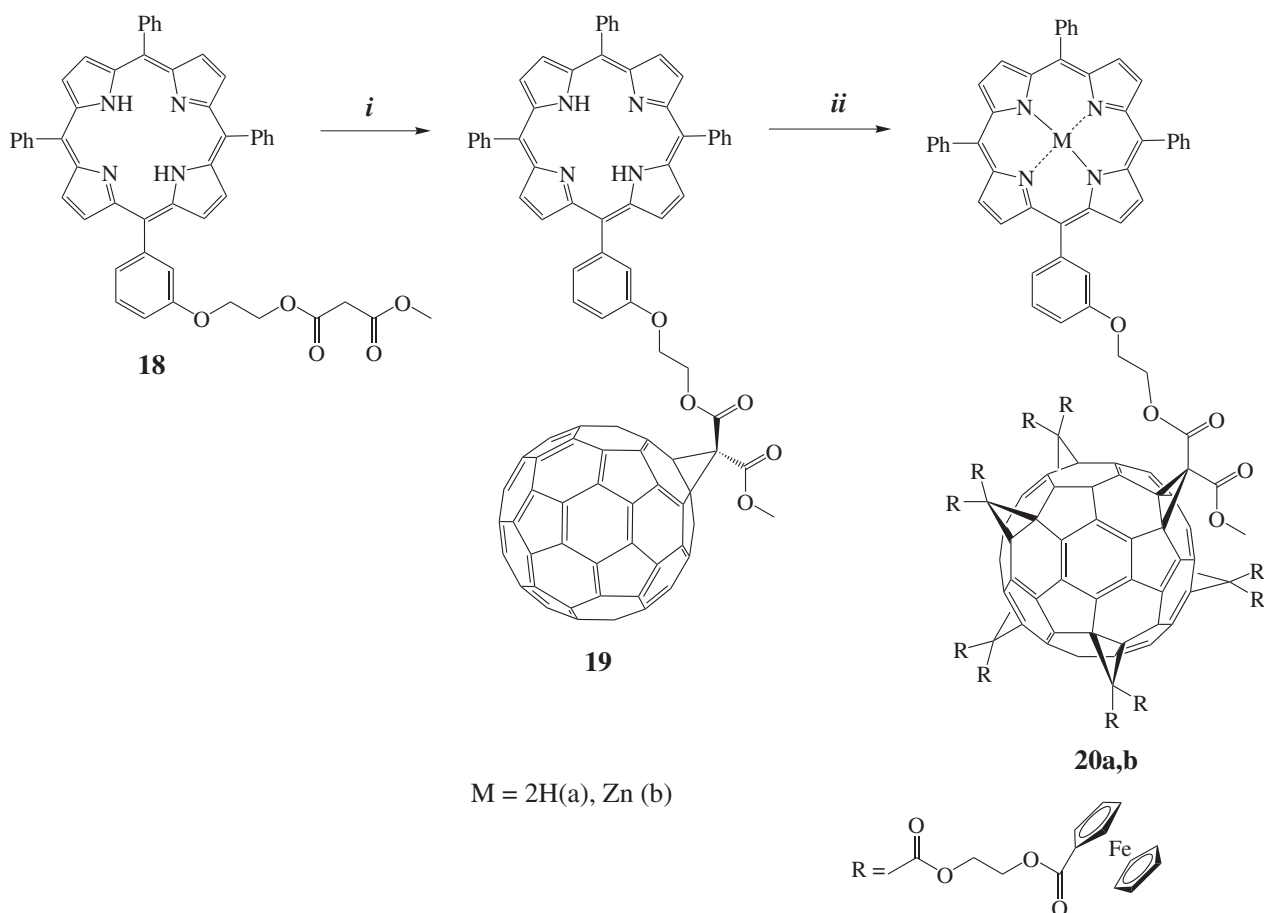


**Scheme 10.** Synthesis of porphyrin – C$_{60}$ conjugate with 12 ferrocene moieties. Reagents and conditions: *i* – I$_2$, DBU, C$_{60}$, toluene; *ii* - DMA, DBU, CBr$_4$, CH$_2$R$_2$, toluene (a); Zn(OAc)$_2$, THF, reflux (b).
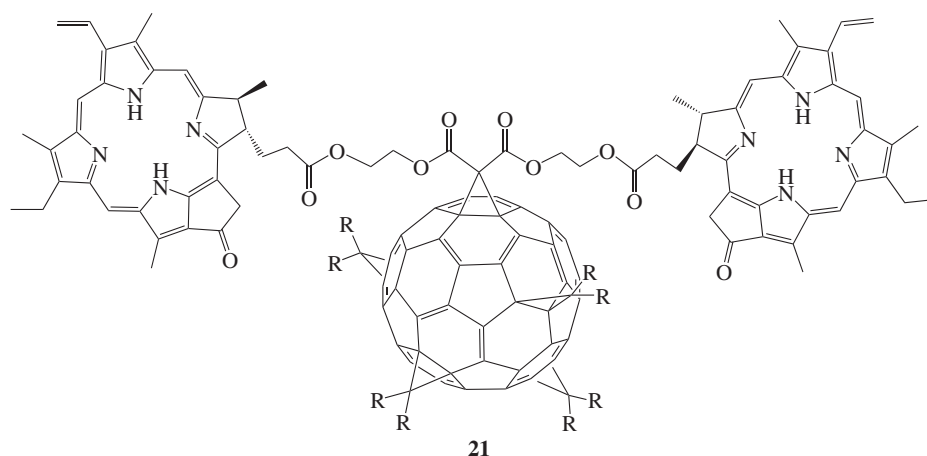


**Figure 4.** Structure of bis-pyropheophorbide *a* – C$_{60}$ conjugate.
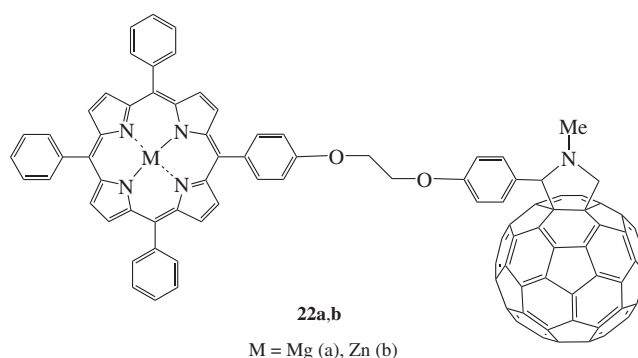
**22a,b**

M = Mg (a), Zn (b)

**Figure 5.** Structure of donor-acceptor systems with a flexible linker **22a** and **22b**.
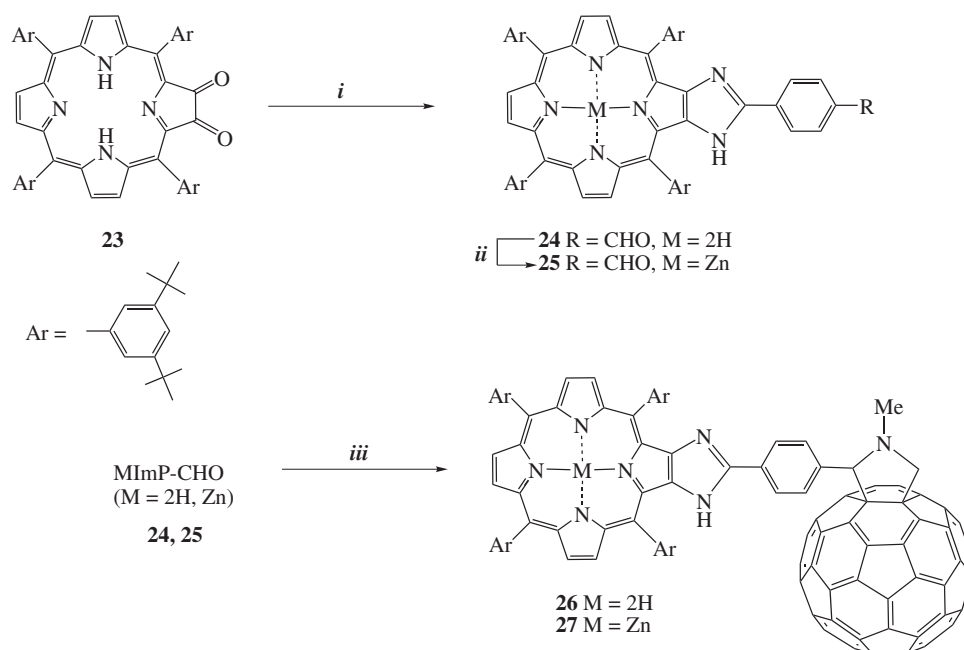
Dyads **22a,b** (Figure 5), containing magnesium and zinc porphyrins were produced in such a way, the central metal ion influence on the photoinduced charges' separation and their recombination was studied.[51,52] The initial 5-(4'-hydroxyphenyl)-10,15,20-triphenylporphyrin was treated with 4-bromoetoxybenzaldehyde in the presence of $K_2CO_3$ to synthesize the corresponding porphyrin-fullerene with a flexible linker and the formyl-containing derivative obtained was condensed with *N*-methylglycine and $C_{60}$ to give porphyrin-fullerene **22**.

In the course of study of the metal complexes obtained the electron transfer from porphyrin to fullerene was shown to yield the charge-separated state $MP^{•+}-C_{60}^{•-}$. Efficient quenching of the excited singlet state ZnP and MgP was revealed. The electron transfer to $C_{60}$ at the rate constant of $2.2 \cdot 10^9$ s$^{-1}$ occurred when quenching the ZnP singlet state,[36] with the MgP singlet state quenching including energy transfer to $C_{60}$ and generating the excited singlet state $C_{60}$ with subsequent charge separation (the rate constant was $1.7 \cdot 10^9$ s$^{-1}$).[52] The rate constant of charge recombination

(lifetime of the charge-separated state) for the compound **22a** was $1.8 \cdot 10^6$ s$^{-1}$ (560 ns) and for the compound **22b** – $3.3 \cdot 10^6$ s$^{-1}$ (300 ns).

The preparation of the porphyrin – fullerene dyad **27** (ZnImP–$C_{60}$) (Scheme 11) with a short linker allowed to prolong the charge-separated state lifetime up to 310 μs in benzonitrile at 278 K.[53] The corresponding formyl porphyrin **24** was produced by condensation of porphyrin-2,3-dion **23** with arylaldehyde in the presence of $NH_4OAc$ when boiled in the mixture AcOH-CHCl$_3$ (1:1), it being transformed into metal complex **25**. The Prato reaction was used for the porphyrin-fullerene **27** production. The dyad's yield was 46 %.

The presence of the photoinduced electron transfer for the dyad ZnImP–$C_{60}$ **27** was confirmed by the picosecond time-resolved absorption spectrum. The rate constant of electron transfer from $^1$ZnImP* to $C_{60}$ was $1.6 \cdot 10^6$ s$^{-1}$. According to the authors, the charge-separated state was not found for the dyad containing free-base porphyrin $H_2$ImP–$C_{60}$ **26**.



**23**

Ar =

MImP-CHO
(M = 2H, Zn)

**24, 25**

**24** R = CHO, M = 2H
**25** R = CHO, M = Zn

**26** M = 2H
**27** M = Zn

**Scheme 11.** Synthesis of porphyrin – fullerene dyad **27**. Reagents and conditions: *i* – arylaldehyde, $NH_4OAc$, AcOH/CHCl$_3$; *ii* – Zn(OAc)$_2$; *iii* - *N*-methylglycine, $C_{60}$, toluene, reflux.

The dyad chlorin–fullerene **30** was synthesized using the Prato reaction.[54] Chlorin–fullerene **29a** was obtained by heating 3-formylcycloimide **28** with *N*-methylglycine and $C_{60}$ (Scheme 12), its treatment with zinc acetate giving metal complex **29b.**
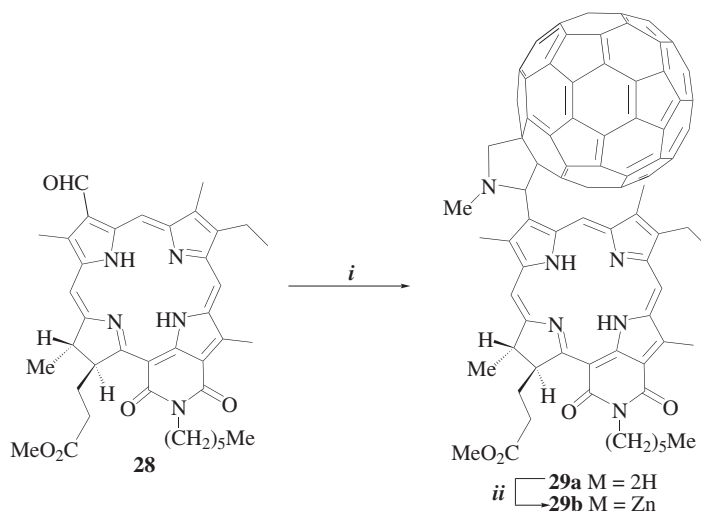
Zinc complex of the chlorin–fullerene dyad **29b** generates extremely long-lived charge-separated state $Zn–Chl^{\cdot+} –C_{60}^{\cdot-}$ with sufficiently high quantum yield (the lifetime is 230 ms at 25 °C and 120 s at –150 °C, the quantum yield of the charge-separated state is 12 %).

It's interesting to note that even slightly less close contact between $C_{60}$ and chlorin macrocycle in dyad **30** results in the reduction of the charge-separated state lifetime to 110 ms (Figure 6) (at 25 °C).[55]

## 2.2. Triads, Tetrads, Pentads, Hexads, Containing Porphyrins and Fullerene $C_{60}$

The triad **31** was constructed using the concept of multistep electron transfer in the natural photosynthesis (Figure 7).[56] The structure involved consisted of diarylporphyrin, carotenoid polyene and fullerene. In this system porphyrin is the initial donor of energy or electron, carotenoid being a secondary electron donor, fullerene acting as an acceptor. This construction was supposed to allow reducing the charge recombination speed and increasing the charge-separated state lifetime.

Formyl-containing porphyrin derivative was synthesized preliminarily to obtain the triad **31**. To achieve this the initial 5-(4-aminophenyl)-15-(4-methoxycarbonyl)phenyl-2,8,12,18-tetraethyl-3,7,13,17-tetramethylporphyrin was turned into a corresponding benzyloxycarbonyl derivative. The ester was reduced with lithium aluminum hydride and the alcohol formed was oxidized by manganese dioxide. The formylporphyrin obtained interacted with sarcosine and $C_{60}$ to form porphyrin-fullerene. The triad **31** was obtained after its treatment with boron tribromide and carotene acid chloride.



**Scheme 12.** Synthesis of chlorin–fullerene $C_{60}$ dyad **29a** and its metal complex **29b**. Reagents and conditions: *i* - *N*-methylglycine, $C_{60}$, toluene, reflux; *ii* – $Zn(OAc)_2$/MeOH.
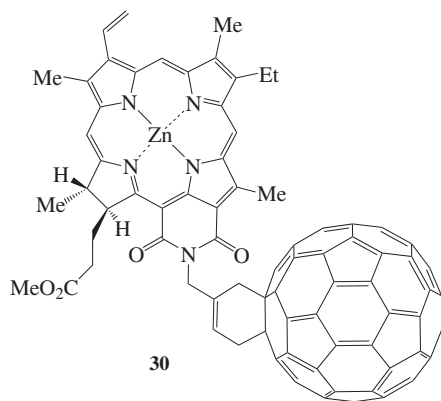


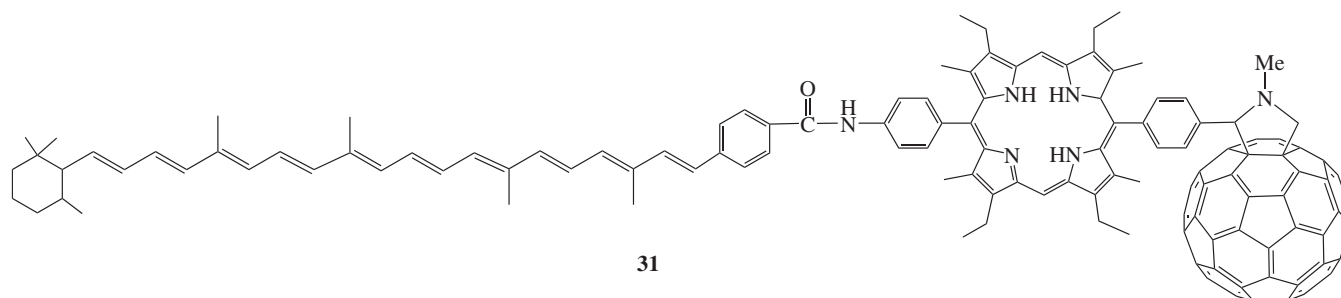**Figure 6.** Structure of chlorin–fullerene **30**.



**Figure 7.** Structure of porphyrin–carotenoid polyene–$C_{60}$ triad **31**.

Photoexciting the triad **31**, electron transfer from porphyrin to fullerene occurred in 2-methyltetrahydrofuran, with an intermediate charge-separated state being formed ($C–H_2P^{\bullet+}–C_{60}^{\bullet-}$), and further hole transfer from porphyrin to carotenoid, charge-separated state being formed ($C^{\bullet+}–H_2P–C_{60}^{\bullet-}$) with a quantum yield 0.14.[56] Charge-separated state lifetimes were 170 ns (in a solution) and 1.5 µs (in a glass matrix at 77 K). However the authors noted that the quantum yield of the long-lived charge-separated state in the triad **31** ($C^{\bullet+}–H_2P–C_{60}^{\bullet-}$) still concedes to the analogous characteristics in the natural photosynthesizing reaction center.

The triad zinc porphyrin–free-base porphyrin–fullerene **39** was synthesized applying the same concept of the multi-step electron transfer (Scheme 13).[57] Synthetic intermediate **33** was obtained by the condensation of dipyrrolylmethane with 3,5-di-*tert*-butylbenzaldehyde in the presence of $BF_3 \cdot OEt_2$ and subsequent alkali hydrolysis of the compound **32** (Scheme 13). The incorporation of zinc atom into diporphyrin and the protection of the latter against demetal-lation appeared to be an important step in the $ZnP-H_2P-C_{60}$ synthesis, subsequent synthesis stages being carried out under neutral or alkaline conditions. Porphyrin diacid **33** was being transformed into the corresponding bis-acid chloride **34**. The cross-condensation of zinc porphyrin **35**, diacid chloride **34** and 4-*tert*-butyldimethylsilyloxymethylaniline in benzene in the presence of pyridine yielded porphyrin mixture. Diporphyrin **36** was isolated (in 34 % yield) after the chromatographic separation of the latter. Compound **37** resulted from the elimination of the *tert*-butyldimethylsilyl group in the compound **36** by treatment with *n*-Bu$_4$NF, it being oxidized with manganese dioxide to form the deriva-tive **38**. $ZnP-H_2P-C_{60}$ **39** was synthesized by the Prato reac-tion *via* the interaction of the compound **38**, *N*-methylglycine and $C_{60}$ in toluene with 79 % yield.

The charge-separated state $ZnP^{\bullet+}–H_2P–C_{60}^{\bullet-}$ was gen-erated under the triad **39** photoexcitation resulting from the electron transfer towards fullerene (quantum yield 0.4 and lifetime 21 µs).[57]
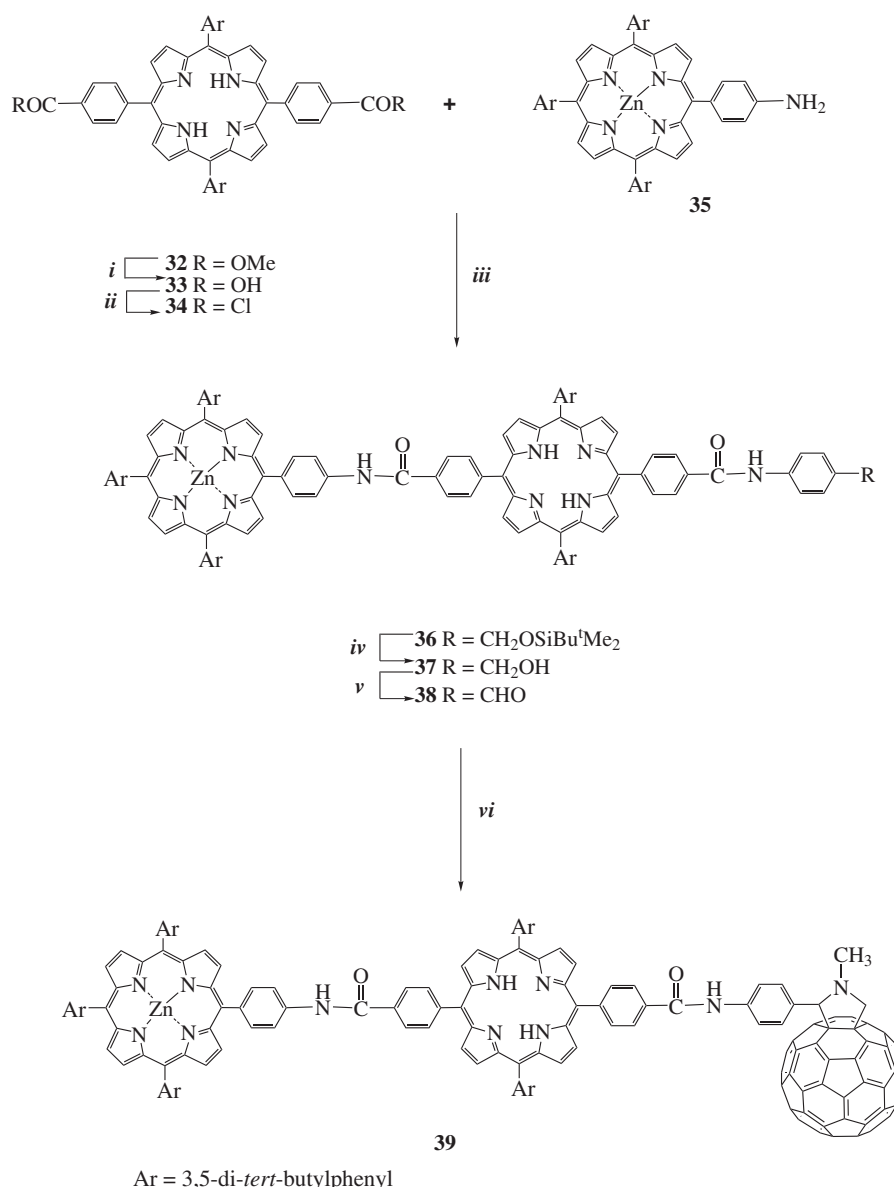


**Scheme 13.** Synthesis of triad **39**. Reagents and conditions: *i* – KOH, THF, EtOH; *ii* – SOCl$_2$, pyridine; *iii* - NH$_2$C$_6$H$_4$CH$_2$OSi(Me)$_2$CMe$_3$, pyridine, benzene; *iv* – Bu$_4$NF; *v* –MnO$_2$; *vi* –*N*-methylglicine, C$_{60}$, toluene, reflux.

The authors[58] introduced ferrocene (Fc) into the triad structure **39** as the third electron donor and synthesized the tetrad Fc–ZnP–H$_2$P–C$_{60}$ **40** (Figure 8). One could observe the energy transfer from zinc porphyrin singlet-excited state to the free-base porphyrin, and then the electron transfer from the porphyrin singlet-excited state to fullerene, primary charge-separated state (Fc–ZnP–H$_2$P$^{\bullet+}$–C$_{60}$$^{\bullet-}$), the hole migration from H$_2$P$^{\bullet+}$ to ZnP giving an intermediate charge-separated state (Fc–ZnP$^{\bullet+}$–H$_2$P–C$_{60}$$^{\bullet-}$), the hole migration from ZnP$^{+}$ to Fc yielding long-lived charge-separated state (Fc$^+$–ZnP–H$_2$P–C$_{60}$$^{\bullet-}$) with a lifetime of 380 ms (benzonitrile, 193 K), which is significantly larger than the initial triad charge-separated state lifetime (21 µs). Such a long-lived charge-separated state is comparable with the processes proceeding in the bacterial photosynthetic reaction center.

To increase the light harvesting efficiency and charge separation pentad Fc–(ZnP)$_3$–C$_{60}$ **41** was constructed (Figure 9), its three molecules of zinc porphyrin serving as light harvesting chromophores.[59] The final charge-separated state Fc$^+$–(ZnP)$_3$–C$_{60}$$^{\bullet-}$ in this case had the lifetime of 0.53 s in dimethylformamide at 163 K and relatively high charge separation efficiency in benzonitrile (the quantum yield 0.83).

The authors[60] succeeded in achieving a long charge-separated state lifetime, having synthesized the triad Fc–ZnP–C$_{60}$ **45** (Scheme 14). The electron donor ferrocene and the acceptor C$_{60}$ in this triad are linked through imidazole rings located at the opposite β,β'-pyrrole sites of zinc porphyrin macrocycle. The compound **44** was produced due to the interaction of tetraone **42**[61] with ferrocene-carboxaldehyde in the presence of ammonium acetate upon boiling in the mixture CHCl$_3$–AcOH (5:1) with subsequent condensation of the dion formed **43** with terephthaldehyde and Zn(II) introduction. The condensation with fullerene C$_{60}$ gave a triad **45** with 73 % yield. The study of photophysical properties of the structure obtained demonstrated that the electron transfer to C$_{60}$ results from porphyrin excitation with the subsequent hole transfer to ferrocene forming long-lived charge-separated state, its lifetime being 630 µs (benzonitrile, 20 °C). The electron transfer rate constant amounted to 4.3·10$^9$ s$^{-1}$. The charge-separated state production Fc$^+$–ZnP–C$_{60}$$^{\bullet-}$ was verified by nanosecond laser flash photolysis technique.

The development of antenna molecular systems with non-linear chromophore arrangement provides the excitation energy transfer to the reaction center of several peripheric chromophores at once.[62,63] The pentad (ZnP)$_3$–H$_2$P–C$_{60}$ **46** is one of the examples of such an approach (Figure 10). The charge-separated state lifetime for this system amounted to 460 ns in the viscous agar medium. The necessity to use the viscous medium resulted from the presence of ester bonds between the structural compounds in the molecule **46**. The presence of flexible linkers resulted in undesirable electronic interactions and the charge-separated state lifetime reduction.
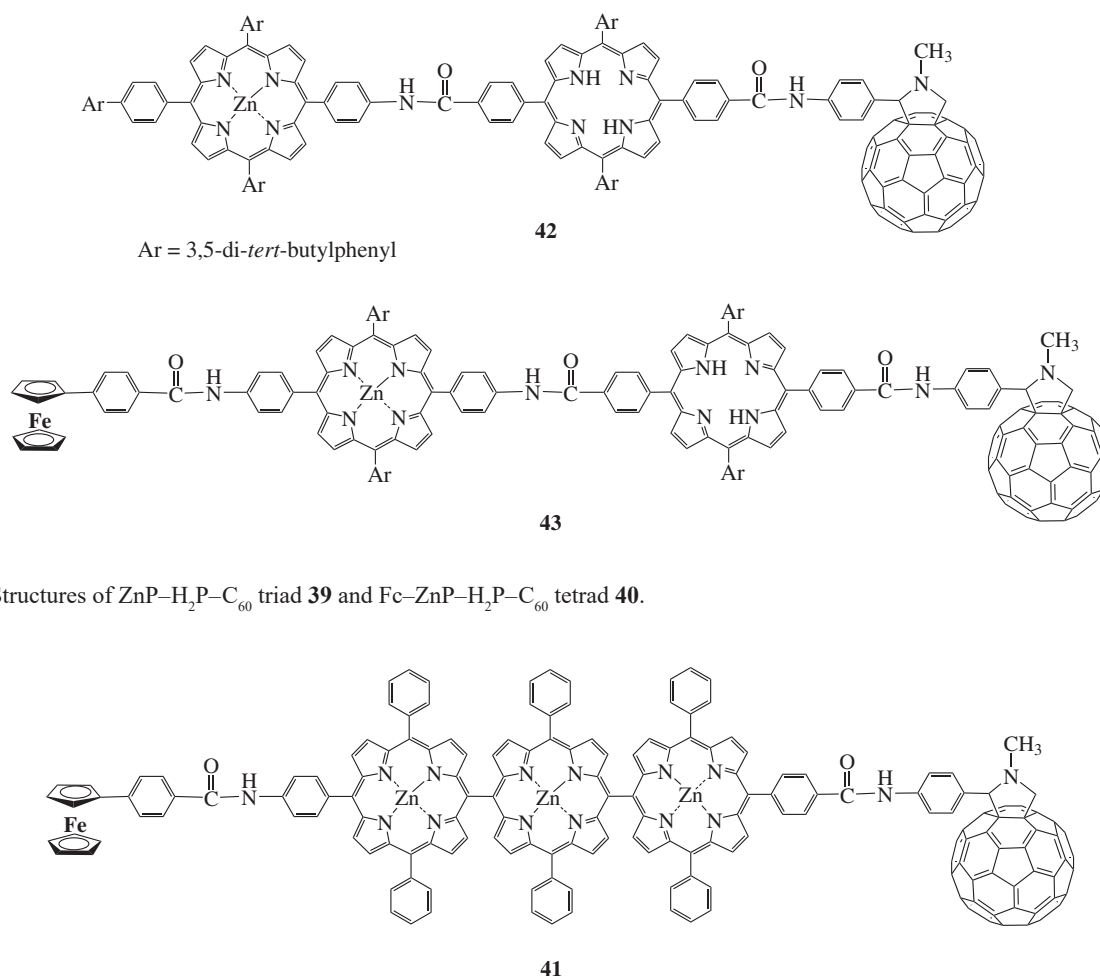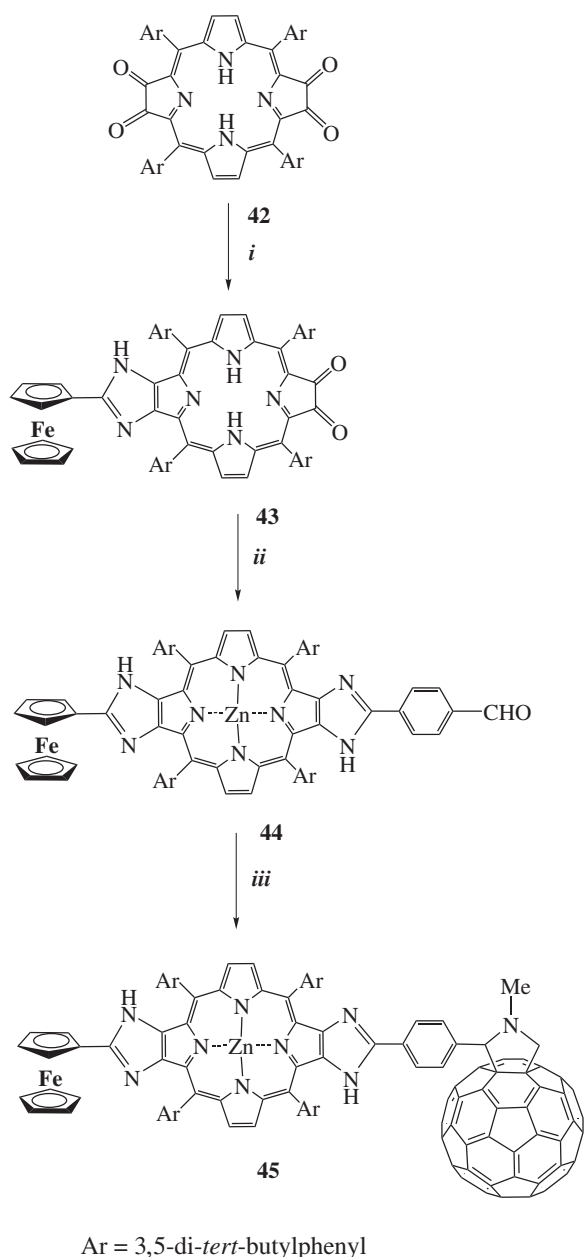


**42**

Ar = 3,5-di-*tert*-butylphenyl



**43**

**Figure 8.** Structures of ZnP–H$_2$P–C$_{60}$ triad **39** and Fc–ZnP–H$_2$P–C$_{60}$ tetrad **40**.



**41**

**Figure 9.** Structure of Fc–(ZnP)$_3$–C$_{60}$ pentad.

**42**

*i*

**43**

*ii*

**44**

*iii*

**45**

Ar = 3,5-di-*tert*-butylphenyl

**Scheme 14.** Synthesis of Fc–ZnP–C$_{60}$ triad **45**. Reagents and conditions: *i* – ferrocenecarboxaldehyde, NH$_4$OAc, CHCl$_3$–AcOH (5:1), reflux; *ii* – Zn(OAc)$_2$, CH$_2$Cl$_2$–MeOH (3:1), reflux (a), terephthalaldehyde, NH$_4$OAc, CHCl$_3$–AcOH (5:1), reflux (b); *iii* – *N*-methylglycine, C$_{60}$, toluene, reflux.

To synthesize the porphyrin tetrad **47** (Figure 11) the Sonogashira reaction was implemented. The coper-free reaction conditions were selected, which allowed to avoid the metalloporphyrins formation. The tetrad **47** was brought about, the yield being 67 %. It was further transformed into a corresponding alcohol for the subsequent malonic acid attachment.

The pentads **48**–**51** were prepared by the author,[64] containing alkyl substituents of different lengths, as well as dendron Newcome of the first and second generations (Figures 12 and 13). Zinc porphyrins in the compounds obtained acted as efficient electron donors, and the central porphyrin molecule acted as a secondary electron donor for C$_{60}$. Rigid binding of porphyrins by means of triple bonds was imple-

mented to prolong the charge-separated state lifetime. Additional substituents were introduced to improve solubility in different media, as well as inhibition of the intramolecular interactions between porphyrins and C$_{60}$.

Pentads containing dendrons moieties **50** and **51** were successfully prepared through the interaction between the synthesized porphyrin-malonate with C$_{60}$ under the Bingel-Hirsh reaction conditions. The hydrolysis of *tert*-butyl ester groups was carried out by treatment of the compounds **50a** and **51a** TMSOTf in 2,6-lutidine.

The photophysical characteristics of the pentads **48**, **49** and **51a** were studied. The electron transfer occurred in the systems involved under photoexcitation in the Soret band region, forming the charge-separated state (ZnP)$_3$–H$_2$P$^{\bullet+}$–C$_{60}^{\bullet-}$. The solvent's nature was shown to play an important role in this process. The electron transfer in benzonitrile proceeded in less than 10 ps, while in toluene in 70–100 ps. The structure of side substituents doesn't influence significantly the charge separation process.

The molecular system **54** was designed to reduce the charge recombination rate.[65] The previously described tetrad **52** was applied as an initial compound in its synthesis (Figure 14). [63,65] The pentad **53** resulted from the palladium catalyzed interaction of the compound **52** with 5-(4-formylphenyl)-15-(4-iodinephenyl)-10,20-dimethylporphyrin, the compound **54** resulting from the pentad **53** under the Prato reaction conditions.

It was stated that under the photoexcitation conditions of the compound **54** in 2-methyltetrahydrofuran the electron transfer occurs from the singlet excited state H$_2$P towards C$_{60}$, generating charge-separated state (ZnP)$_3$–H$_2$P$^{\bullet+}$–C$_{60}^{\bullet-}$, its lifetime being 25 ps, quantum yield being 0.98.[65] The subsequent positive charge migration occurs from H$_2$P$^{\bullet+}$ to ZnP, producing the final charge-separated state (ZnP)$_3^{\bullet+}$–H$_2$P–C$_{60}^{\bullet-}$, its lifetime being 240 ns, which is 100 times the lifetime of the primary charge-separated state.

The pentad **59** consisting of three BODIPY (BDP) fragments (antenna), zinc porphyrin (energy acceptor and electron donor) and C$_{60}$ (electron acceptor) is the example of another similar complex (Scheme 15).[66,67]

The metal complex **55** was synthesized beforehand,[68] then it was treated with 1,3-dibromopropane and 4-hydroxybenzaldehyde in the presence of K$_2$CO$_3$ in DMF to form bromide **56** and aldehyde **57**. The porphyrin-fullerene **58** was synthesized by the interaction of the derivative **57** with *N*-methylglycine and C$_{60}$ *via* the Prato reaction.

Click-reaction was applied at the final step of the synthesis – Cu(I)-catalyzed 1,3-dipolar cycloaddition between the azides and alkynes. The alkyne-containing porphyrin-fullerene **58** interacted with azide-BDP in the presence of sodium ascorbate and CuSO$_4$·5H$_2$O forming the pentad (BDP)$_3$–ZnP–C$_{60}$ **59** with 88 % yield.

The compound **59** absorbs in a wide range of wavelengths (from 300 to 700 nm). Overlapping of the emission spectra of BODIPY and the absorption of ZnP leads to energy transfer from the singlet-excited state of BODIPY to ZnP with a sufficiently large rate constant of 2.7·10$^{10}$ s$^{-1}$. The further electron transfer from ZnP to C$_{60}$ resulted in charge-separated state (BDP)$_3$–ZnP$^{\bullet+}$–C$_{60}^{\bullet-}$ with the rate constant being 1.7·10$^{11}$ s$^{-1}$, the charge recombination rate constant
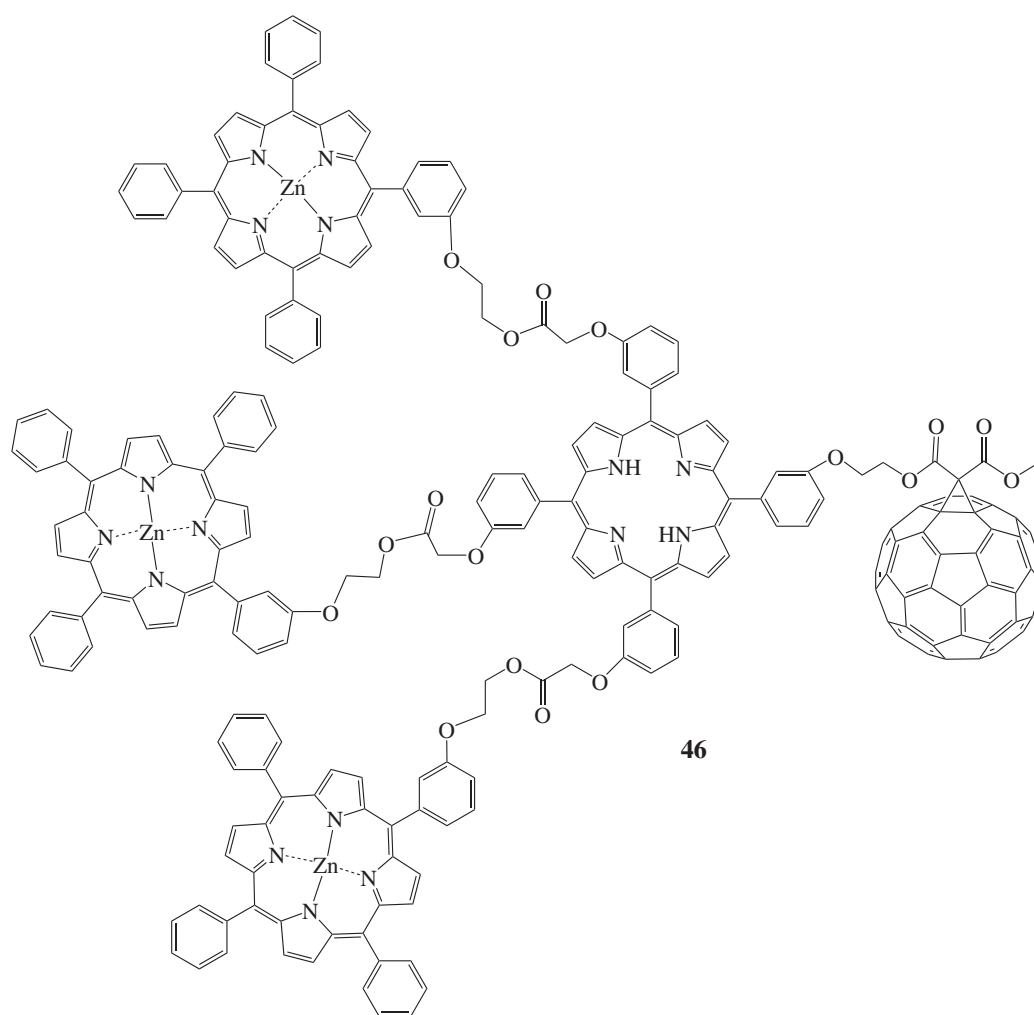
**Figure 10.** Structure of (ZnP)$_3$–H$_2$P–C$_{60}$ pentad **46**.

amounting to $1.0 \cdot 10^9$ s$^{-1}$, the lifetime of charge-separated state being 1 ns.

The structure consisting of two triphenylamide moieties (antenna and electron donor), porphyrin (energy acceptor and electron donor) and C$_{60}$ (acceptor) serves as another example of multistep electron transfer (Scheme 16).[69]

Dipyrromethane **63** was condensed with 4-(diphenylamino)benzaldehyde **64** in the presence of BF$_3 \cdot$OEt$_2$ with subsequent oxidation with *p*-chloranil. Having neutralized the reaction mixture with triethylamine the product **62** was hydrolyzed under alkaline conditions to form 5,15-di(*p*-carboxyphenyl)-10,20-di(triphenylamine)porphyrin **63**. The compound **63** was turned into acid chloride, which interacted with formyl-substituted aniline and then with 4-ferrocenylaniline to produce the porphyrin **64**. The latter reacted with *N*-methylglycine and C$_{60}$, zinc was incorporated into the polyad produced **65a** (the compound **65b**).

The singlet-singlet energy transfer from triphenylamine to ZnP and the electron transfer from ZnP to C$_{60}$ was observed when the polyad **65b** was illuminated in the ultraviolet region of spectrum. In this transition state Fc–ZnP(TPA)$_2$·$^+$–C$_{60}$·$^-$ the hole transfer from ZnP to Fc occurs to form the final charge-separated state Fc–ZnP(TPA)$_2$·$^+$–C$_{60}$·$^-$, its lifetime being 8.5 μs,[69] which is much greater than that for ZnP(TPA)$_3$–C$_{60}$ **66**[70] (Figure 15).

The Prato reaction was also used when producing the photoconductive nanostructures based on amphiphilic chiral dyad **67**, being photoinduced by light in the visible spectrum region (Figure 16).[71] The dyad **67** was synthesized [3+2] by cycloaddition of porphyrin, containing azide group in the *meso*-phenyl substituent and alkyl-functionalized fullerene C$_{60}$. The compound **67** self-assembles into nanofibers and presents a significant interest for photovoltaics.

Some other amphiphilic dyads **68** and **69** were obtained by the authors,[72] having analogous hydrophilic moiety with triethylene glycol residues, but different linkers between porphyrin and fullerene, self-assembling into nanotubes of varying spacial and geometric structure. The nanotubes, formed by the dyad **68** with an ester bond, had a bi-layer wall with coaxially generated along the tube's axis donor and acceptor domains and possessed a significant photoconductivity. Using the methods of scanning and transmission electronic micrographics it was stated that the nanotubes (diameter 32 nm and wall thickness 5.5 nm) result from self-assembling of the dyad **68**. On the contrary, the dyad **69** with a rigid arylacetylene linker due to self-assembling resulted in nanotubes with a monolayer wall and less regular geometry of the donor and acceptor stacking, bringing about the weakening of photoconductivity.
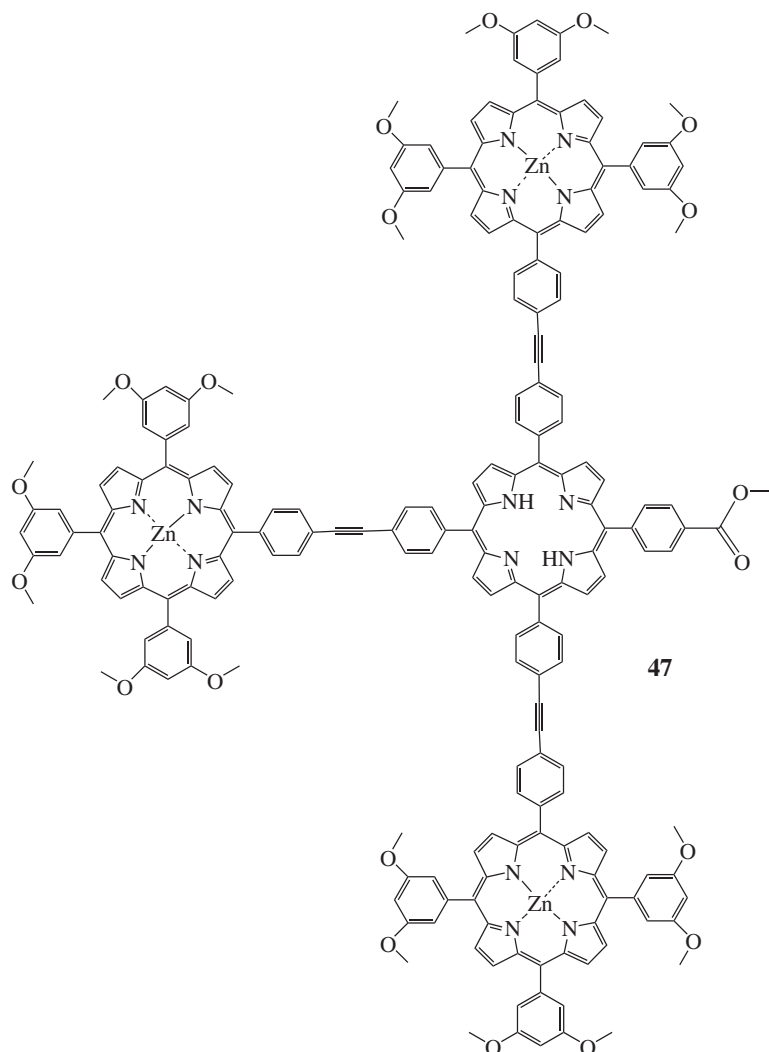
**Figure 11.** Structure of tetrad **47**.

## 3. Porphyrin- and Chlorin-Fullerenes and PDT

The creation of hybrid structures based on porphyrins and chlorins, absorbing intensively in the range of visible spectrum, and fullerenes generating efficiently the active oxygen forms, allows to improve considerably the efficiency of the photosensitizers' photodynamic action. Fullerenes in conjugates have an additional function as transporters. Fullerene lipophilicity facilitates the conjugate transfer across the membrane of the cancer cell.

The photoinduced activity *in vitro* on throat carcinoma cells of man Hep-2 was studied for the dyads **70a** and **70b**, synthesized on the base of tetraphenyl porphyrin and $C_{60}$ derivative, potentially giving an efficient electron transfer (Figure 17).[73] The compound **70a** was produced by the condensation of 5-(4-amydophenyl)-10,15,20-tris(4-metoxyphenyl)porphyrin and 1,2-dihydro-1,2-methane fullerene[60]-61-carboxylate.[74] The metal complex **70b** was synthesized by the dyad **70a** treatment with zinc acetate. The presence of methoxy groups in the porphyrin phenyl cycles as well as Zn in the porphyrin core increased its electron-donor characteristics. As a result of the tests it was stated that both dyads were capable to generate singlet oxygen, demonstrating a significant dependence of its production on the solvent's polarity (0.80 for the compound **70a** and 0.62 for the compound **70b** in toluene and 0.18 and 0.04, respectively, in DMF). The dyads **70a** and **70b** were accumulated in the cells Hep-2 in less than 4 hours. The porphyrin-fullerene phototoxicity was decreasing in the order P-$C_{60}$>ZnP$C_{60}$>P. Inactivation of 80 % cancer cells was observed to take place for P-$C_{60}$ after irradiation during 15 min. The high phototoxic effect was preserved even in the absence of oxygen, and the photoinduced decay of cancer cells for P-$C_{60}$ in the argon medium was higher than for the free porphyrin under aerobic conditions. Depending on microenvironment when the dyads were localized in cancer cells, their photo decay was carried out either by the action of singlet oxygen or under a low oxygen concentration, due to the other active oxygen forms. Under anaerobic conditions the apoptosis process along the caspase-3-dependent pathway (58 % of apoptotic cells) was changed by the prevalence of necrotic phenomena. Thus, it was shown that the molecular systems synthesized, obtaining the photoinduced charge-separated state are promising models for the cancer cells inactivation by the PDT.

Rather high quantum yield of singlet oxygen was observed also for the dyads **71** and **72** (0.62–0.63) with an efficient electron transfer (Figure 18).[75] The dyads
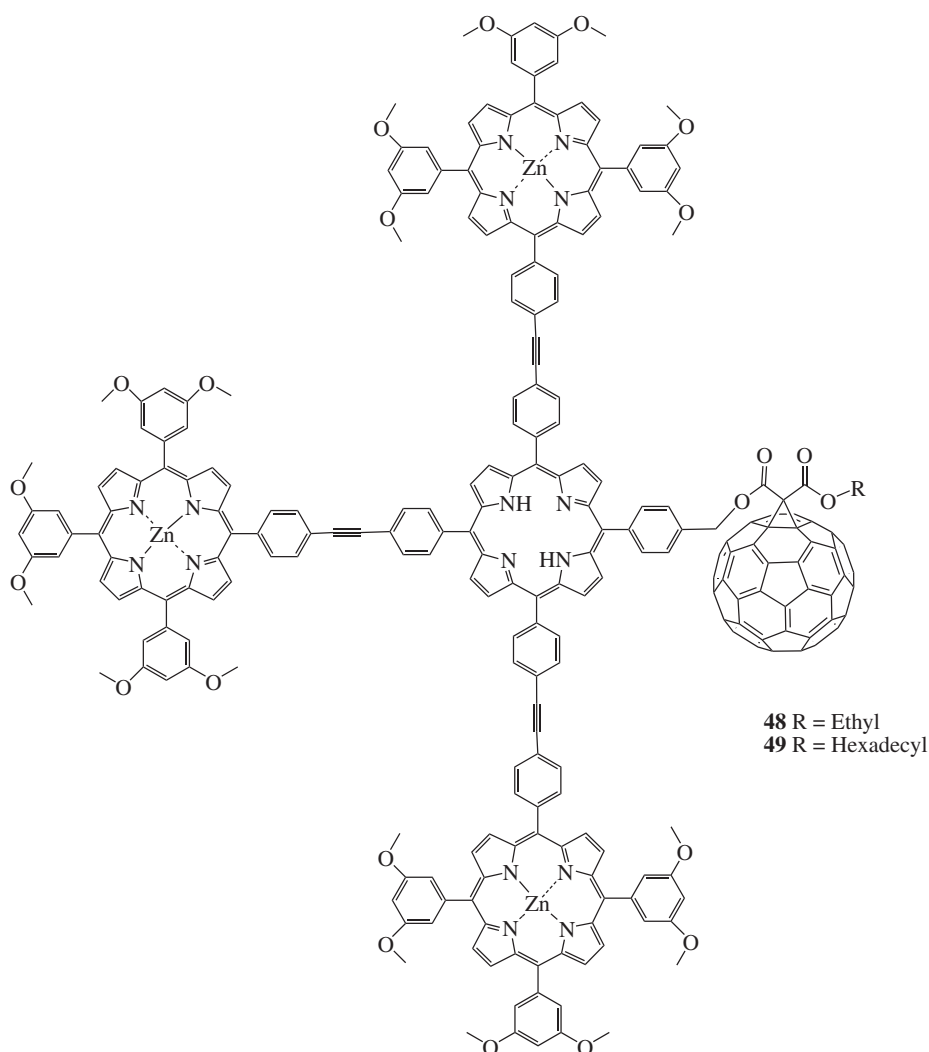
**Figure 12.** Structures of pentads with additional alkyl substituents **48** and **49**.

**71** and **72** were synthesized by the interaction of the corresponding hydroxyiminomethyl substituted derivatives of chlorin $p_6$ cycloimide with $C_{60}$ in the presence of diacetoxyiodobenzene.[76]

The possibility of porphyrin–fullerene $C_{60}$ dyad **74** application was studied (Scheme 17), containing 3 carbazoyl groups at the *meso*-positions of the tetrapyrrolic macrocycle, and its polycationic derivative **75** for the photodynamic inactivation of the cells *Staphylococcus aureus*.[77] The dyad **74** was produced applying the reaction of 1,3-dipolar linking by the interaction of 5-(4-formylphenyl)-10,15,20-tris[3-(4-ethylcarbazole)]porphyrin **73**, *N*-methylglycine and $C_{60}$. The exhausting dyad methylation with dimethylsulphate yielded the cationic derivative **75**.

The spectroscopic properties of the dyads concerned were studied in homogeneous media of different polarity as well as in a biometric system toluene/sodiumbis(2-ethylhexyl)sulfosuccinate (AOT)/water, forming the reversed micelles. Singlet oxygen production for the compounds obtained depended significantly on the polarity of the solvent. A considerable quantum yield of singlet oxygen generation for the dyad **74** was observed in toluene (0.56), however in a more polar solvent, dimethylformamide, it decreased

significantly (0.01) owing to the stabilization of the charge-separated state. Rather high quantum yield of the singlet oxygen generation was observed for both dyads (0.50 for **74** and 0.46 for **75**) in the biomimetic system.

The photoinactivating power of the dyads **74** and **75** was examined using the *Staphylococcus aureus* cells suspension. When using 5 μm of the dyad **75** and the exposure to light in the range (350–800 nm) during 30 min complete cells inactivation was observed. Under the same conditions lower photo cytotoxic effect was observed for the dyad **74**. The photoinactivation of *Staphylococcus aureus* using the dyad **75** was stated by the authors to be less efficient than when using the cationic derivatives of the parent compounds $DAC_{60}^+$ and $TCP^{4+}$.

A highly water-soluble dyad **78** (Scheme 18) based on chlorin $e_6$ amine derivative **76** and polyanionic derivative $C_{60}$ **77**, possessing high solubility in water, was produced by the authors,[34] and its spectral properties and photochemical activity were studied. Strong quenching of the chlorin fluorescence as well as the dependence of the fluorescence quenching extent on the solvent's polarity indicated an efficient electron transfer from macrocycle to fullerene. The dyad synthesized was stated to possess a pronounced
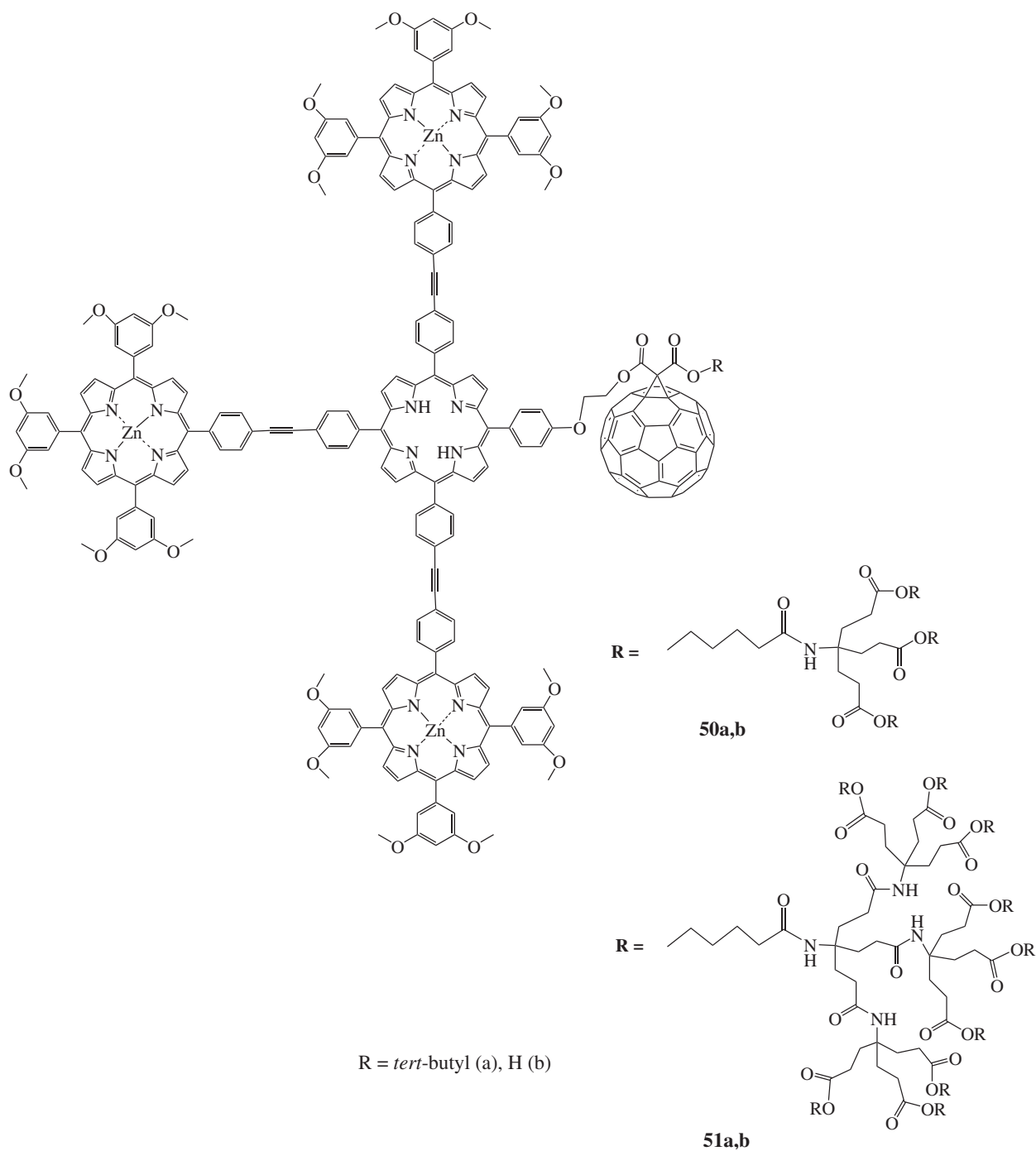
R = *tert*-butyl (a), H (b)

**Figure 13.** Structures of pentads with dendrons moieties **50** and **51**.

photochemical activity more than 10 times that of the free chlorin, which indicates the prospects of water-soluble chlorin-fullerene production as promising photosensitizers for medicine.

Fullerene is known to transform the light energy into vibrational energy causing the temperature increase. In this connection, multimeric conjugate of chlorin $e_6$, folate and $C_{60}$ **79** presents a special interest for application in the combined photothermal/photodynamic therapy of cancer.[78] The conjugate **79** synthesis is shown at the Scheme 19. Chlorin $e_6$ and folate were activated with DCC and *N*-hydroxysuccinimide (NHS) to form the respective succinates. Polyethylene glycol (PEG) was treated with succinic anhydride in the presence of DMAP and TEA and the di-carboxylated PEG deriva-

tive obtained successively interacted with DCC and NHS, and the ethylenediamine excess forming $NH_2$-PEG-$NH_2$. $C_{60}$ reacted with $NH_2$-PEG-$NH_2$, activated with chlorin $e_6$-NHS and folate-NHS to give multidimensional conjugate **79**.

The anticancer activity of multidimensional conjugate was studied both *in vitro* and on the cells of KB human carcinoma with high expression of the folate receptors. The temperature on the tumor's surface of mice with the KB tumor was shown to amount to 44 °C after the conjugate administration. Hyperthermal conditions and high quantum yield of the singlet oxygen generation by multimeric conjugate resulted in a significant regression of the tumor's volume *in vivo*. The conjugate **79** also inhibited efficiently the arthritis development of mice.
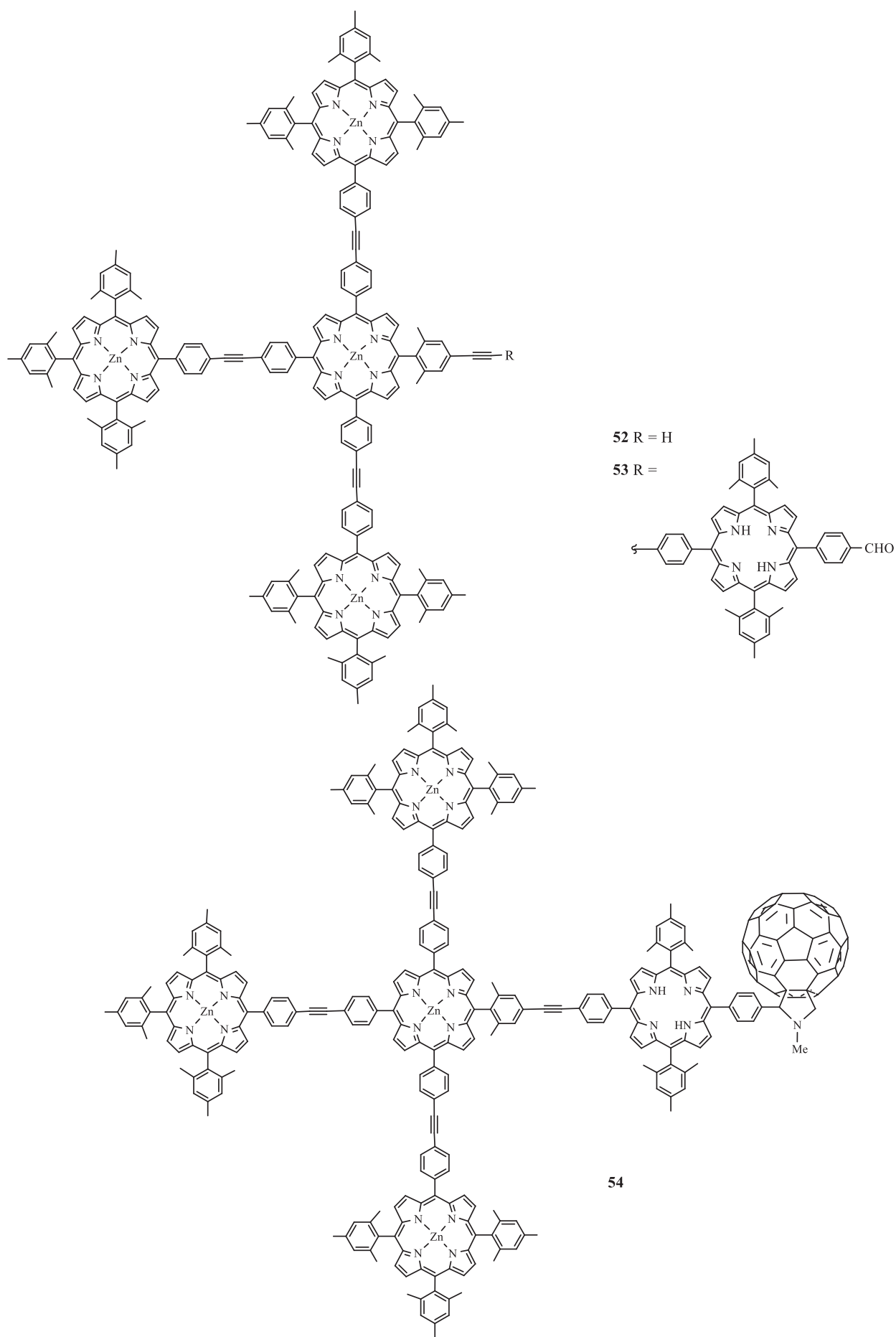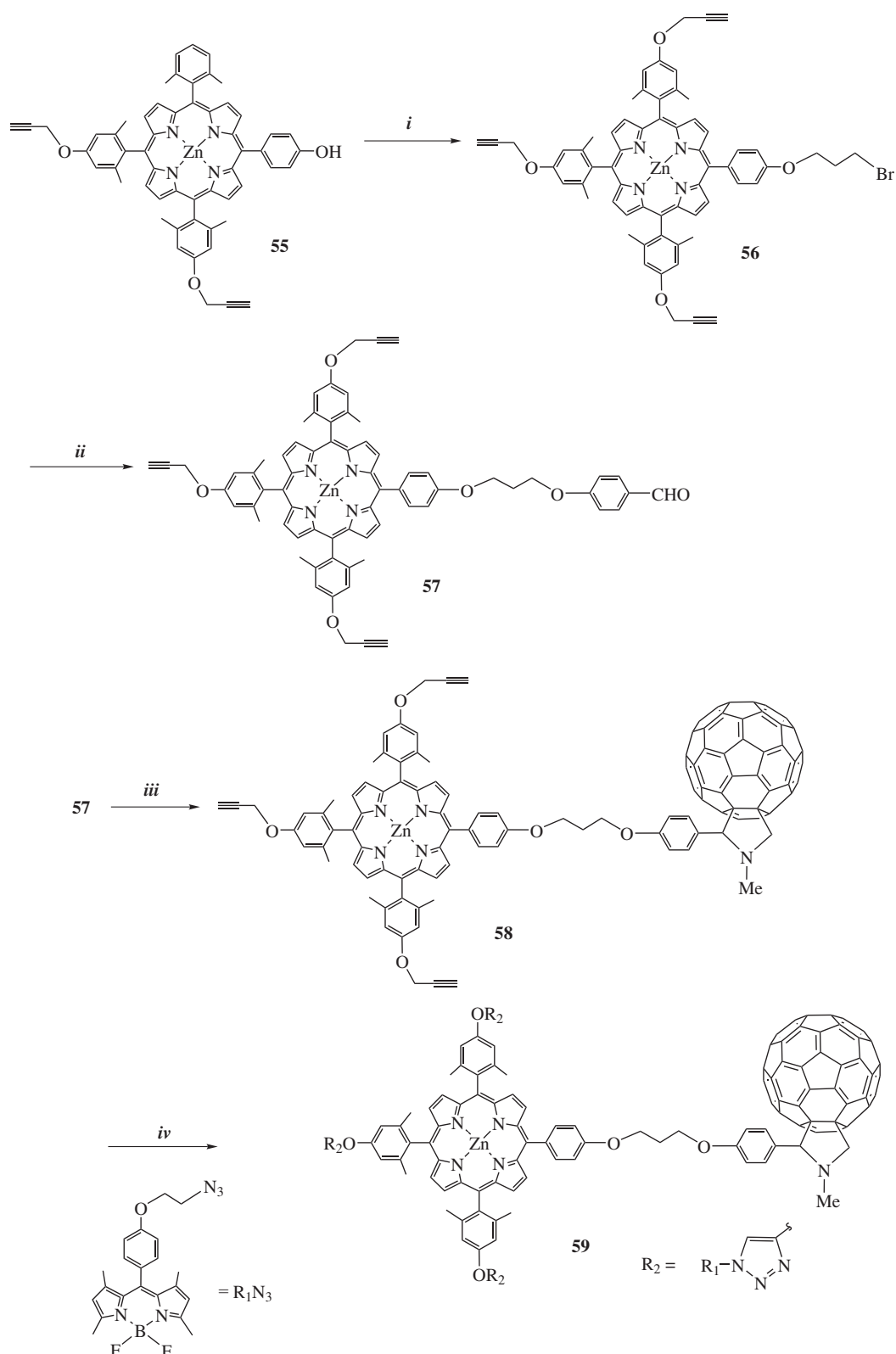
**52** R = H

**53** R =

**54**

**Figure 14.** Structures of tetrad **52**, pentad **53** and molecular system **54**.

**Scheme 15.** Synthesis of pentad **59**. Reagents and conditions: *i* – Br(CH$_2$)$_3$Br, K$_2$CO$_3$, DMF; *ii* – 4-hydroxybenzaldehyde, K$_2$CO$_3$, DMF; *iii* – *N*-methylglycine, C$_{60}$, toluene, reflux; *iv* – R$_1$N$_3$, sodium ascorbate, CuSO$_4$·5H$_2$O, CHCl$_3$/EtOH/H$_2$O (12:1:1).

The conjugate of chlorin $e_6$ with fullerene C$_{70}$ modified with three residues of malonic acid may serve as an example of the efficient phototheranostic nanoplatform for the PDT application with an improved accumulation in tumor cells.[79] The possibility of production of nanovesicles based on amphiphilic fullerene derivatives for diag-nostics and therapy of cancer *in vivo* was demonstrated by the authors for the first time. The amphiphilic conjugate was synthesized by the condensation of chlorin $e_6$ prelimi-nary modified with 1,10-diamino-4,7-dioxadecane (OEG2) with fullerene C$_{70}$ derivative containing three residues of the malonic acid (Scheme 20). The conjugate obtained **80**
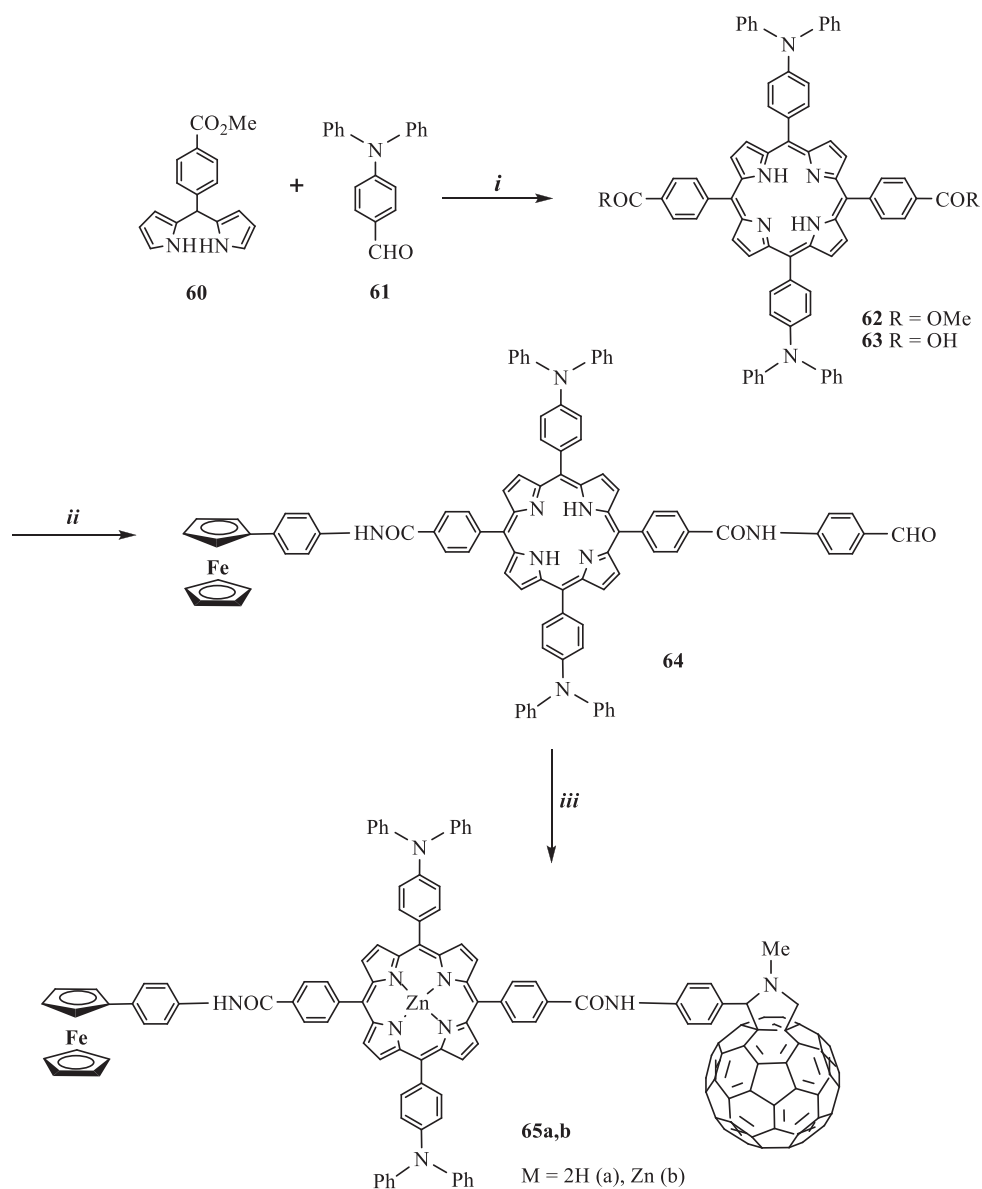
**Scheme 16.** Synthetic pathways for obtaining of polyad **65a** and the metal complex **65b**. Reagents and conditions: *i* – BF$_3$·OEt$_2$, CHCl$_3$ (a), *p*-chloranil (b), KOH, THF/EtOH, reflux (c); *ii* – 4-ferrocenylaniline, SOCl$_2$, pyridine, toluene, reflux (a), formyl-protected aniline (b), H$_2$SO$_4$, TFA, CHCl$_3$ (c); *iii* – *N*-methylglycine, C$_{60}$, toluene, reflux (a), Zn(OAc)$_2$/MeOH (b).
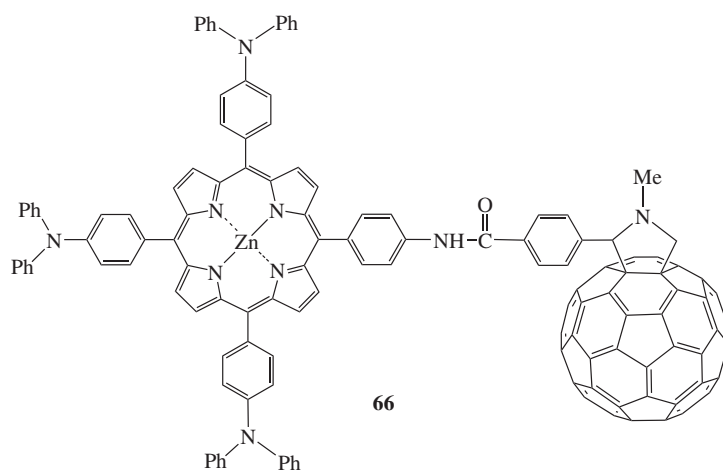
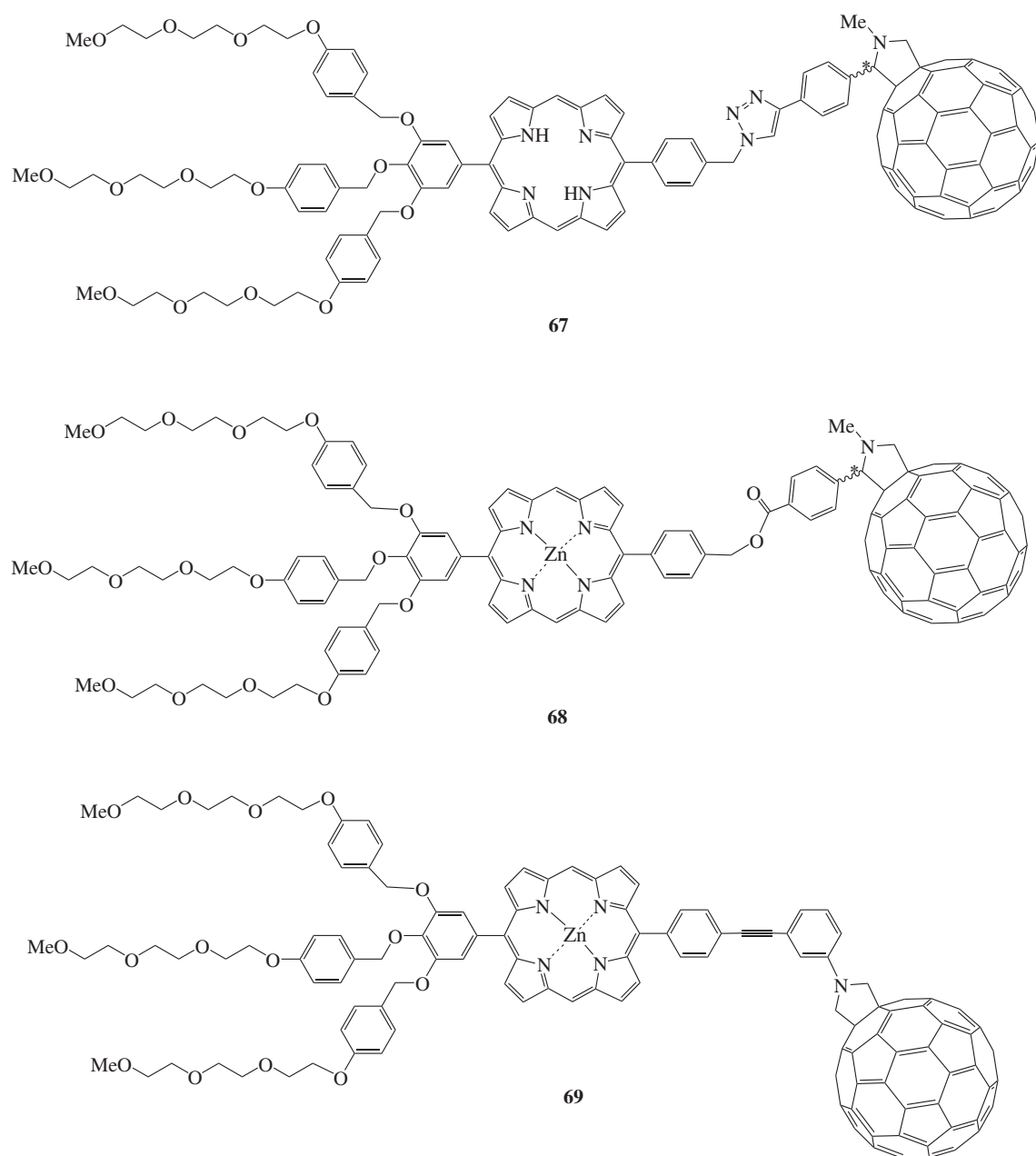

**Figure 15.** Structure of donor-acceptor system **66**.

**67**



**68**



**69**

**Figure 16.** Structures of amphiphilic dyads **67-69**.



**70a,b**

M = 2H (a), Zn (b)



**71**

**72**

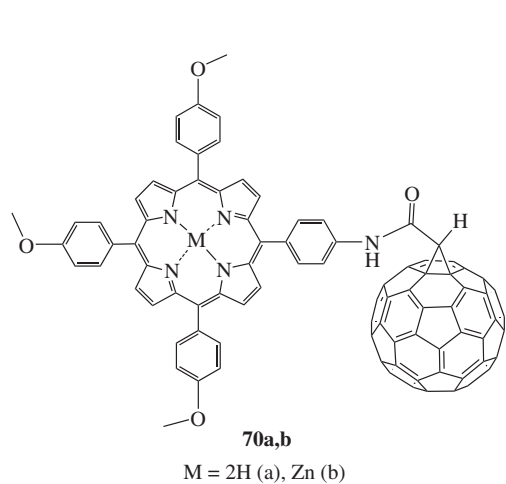**Figure 17.** Structure of dyads obtained from the tetraphenylporphyrin derivative and $C_{60}$.
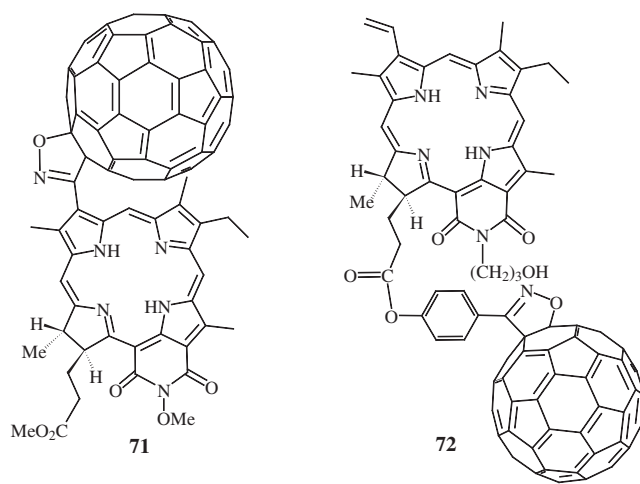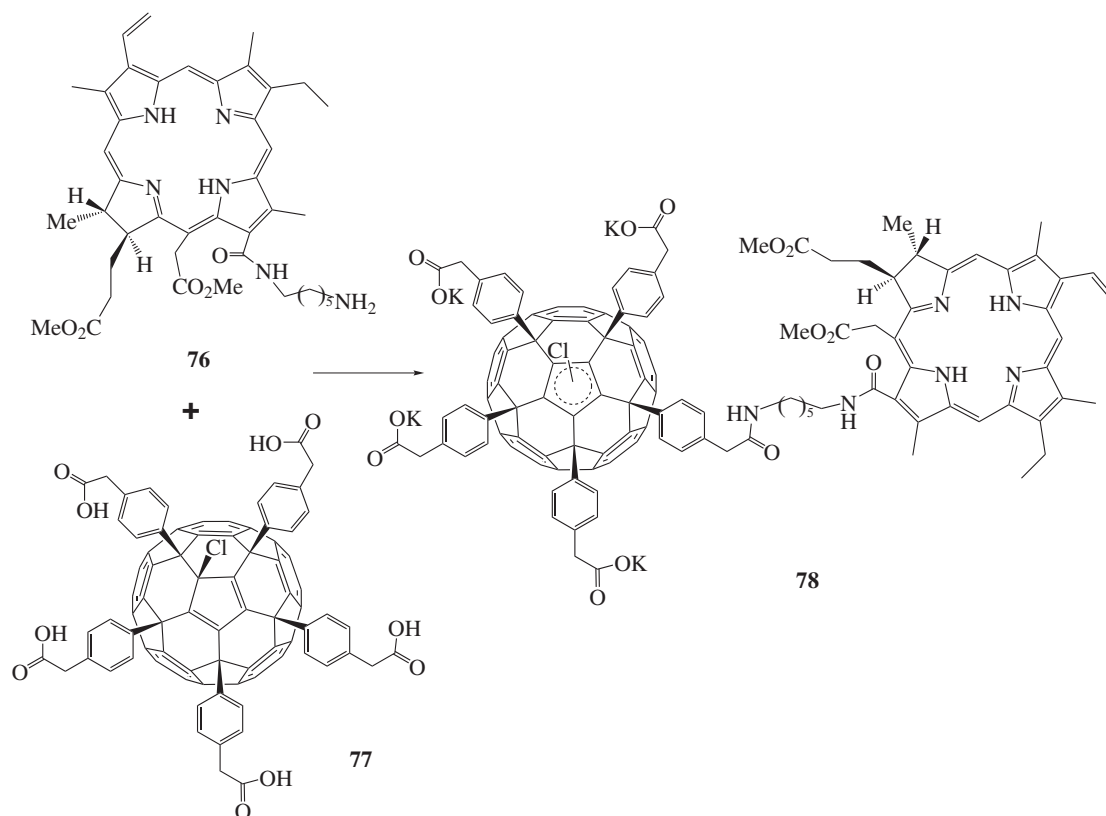
**Figure 18.** Structures of chlorin $p_6$ cycloimide – $C_{60}$ dyads **71** and **72**.
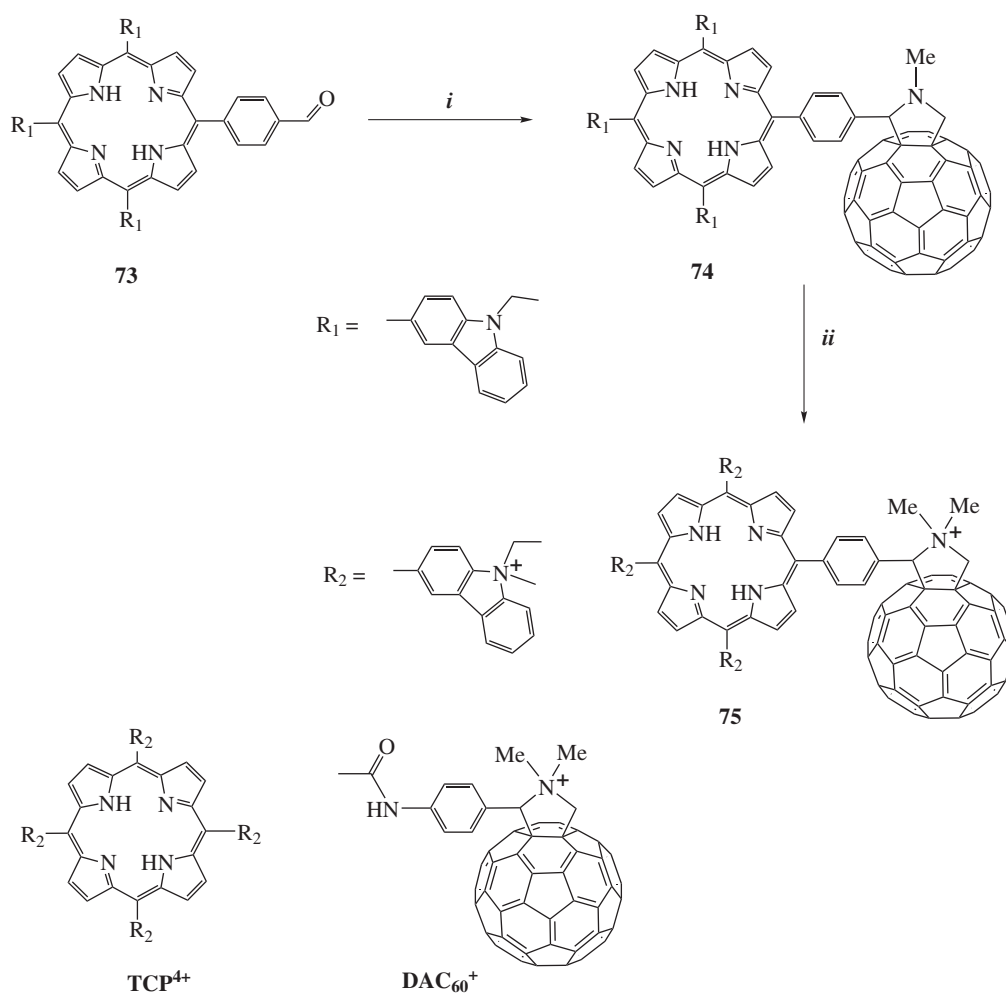
**Scheme 17.** Synthesis of porphyrin–fullerene dyad **74** containing carbazoyl grous and its polycationic derivative **75**.



**Scheme 18.** Water-soluble dyad chlorin–C$_{60}$.
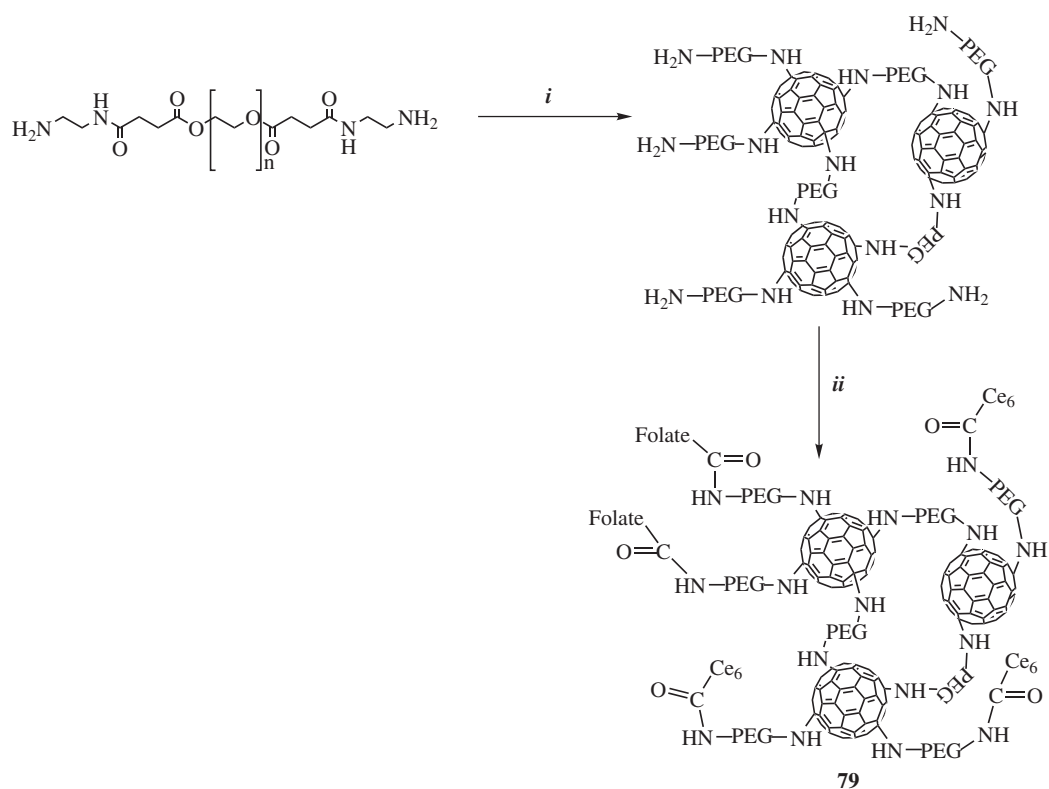
**Scheme 19.** Synthesis of multimeric conjugate **79**. Reagents: *i* – C$_{60}$, benzene; *ii* – Ce$_6$-NHS, folate-NHS.
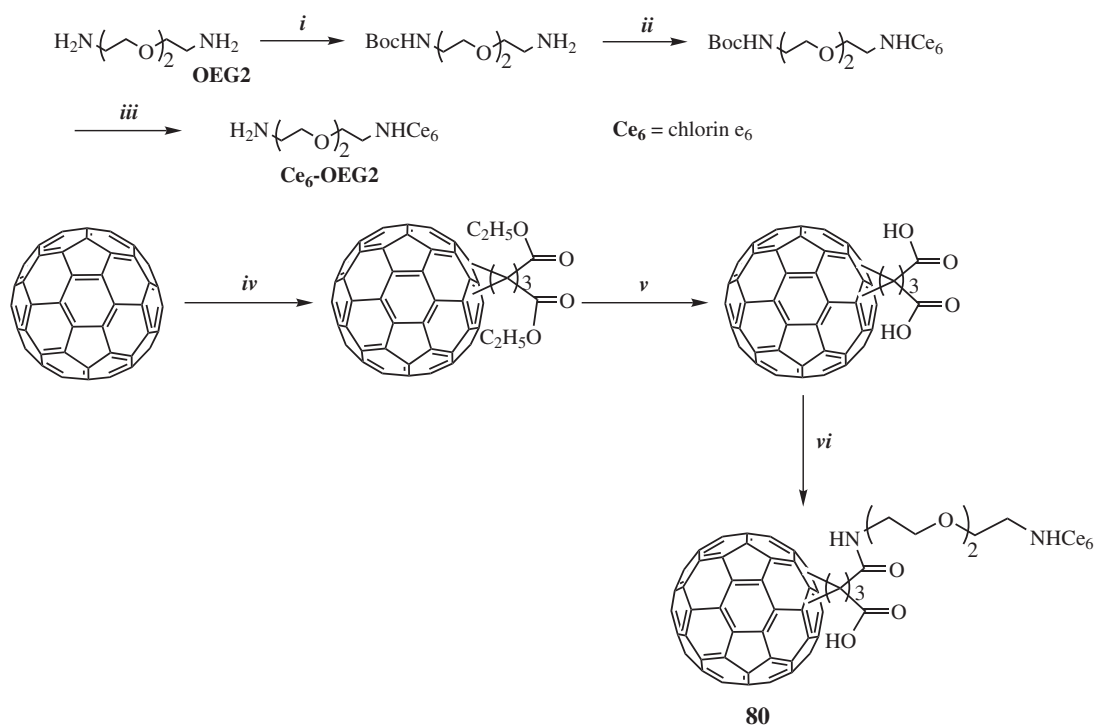


**Scheme 20.** Synthesis of chlorin $e_6$ and C$_{70}$ amphiphilic conjugate **80**. Reagents and conditions: *i* – Boc$_2$O, DCM; *ii* – EDC/NHS, Ce$_6$, DMSO; *iii* – TFA, Na$_2$CO$_3$; *iv* – BrCH(COOC$_2$H$_5$)$_2$, DBU; *v* – NaH; *vi* –EDC/NHS, Ce$_6$-OEG2, DMSO.

formed vesicles with a high chlorin $e_6$ contents (up to 57 %), demonstrated extensive absorption in the long-wave region and accumulated well in the cancer cells of human lung adenocarcinoma A549, exhibiting strong activity *in vivo*, was biocompatible and well eliminated from the organism.

## Conclusions

Thus, the achievements in the field of porphyrin- and chlorin-fullerene synthesis made these compounds available and gave the opportunity to produce a wide range of artificial photosynthetic models beginning with simple dyads and triads till multichromophoric systems in order to study the relations between the structure and photo-chemical activity and to approach to their application when preparing the models to study the mechanism of natural photosynthesis, artificial conversion of solar energy, pho-toelectrical devices. It was shown that the rate and the effi-ciency of the energy and electron transfer are significantly influenced by the alteration of the distance and orientation of the donor- and acceptor-moieties, the nature of solvent and the linker between the photoactive moieties. The quan-tum yields and the charge-separation lifetime are the param-eters, characterizing the progress in artificial photosynthetic systems. The application of the multistep electron transfer concept, which is realized in the natural photosynthesis, along well-defined redox gradients, is one of the effec-tive approaches, which allows to prolong the lifetime of the charge-separated state. The compounds were pro-duced as a result of the design and synthesis of a number of covalently linked porphyrin-fullerene systems, which have a fast charge separation with extremely slow charge recombination and the lifetime of the charge-separated state is comparable and even exceeded the lifetime of the charge-separated state in the natural bacterial photosynthetic reac-tion center.

The use of porphyrin- and chlorin-fullerene structures in medicine are extremely promising. The conjunction of porphyrins and chlorins, absorbing intensively in the vis-ible region of spectrum, and fullerenes, generating various active forms of oxygen efficiently, allows to increase the effi-ciency of the photodynamic effect of the photosensitizer. The examples published witness the prospects of the appli-cation of such compounds in antimicrobial photodynamic inactivation, the combined photothermal/photodynamic therapy of cancer and in phototheranostics.

## References

1. Sanders J.K.M., Bampos N., Clyde-Watson Z., Darling S.L., Hawley J.C., Kim H.-J., Mak C.C., Webb S.J. Axial Coordi-nation Chemistry of Metalloporphyrins. In: *The Porphyrin Handbook* (Kadish K., Smith K.M., Guilard R., Eds.), Vol. *3*, San-Diego, California, London: Academic Press, **2000**. p. 1–48.
2. Guldi D.M., Prato M. *Acc. Chem. Res.* **2000**, *33*, 695–703.
3. Guldi D.M., Asmus K.-D. *J. Am. Chem. Soc.* **1997**, *119*, 5744–5745.
4. Guldi D.M., Fukuzumi S. From Synthesis to Optoelectronic Properties. In: *Fullerenes* (Guldi D.M., Martin N., Eds.) Dordrecht: Kluwer Academic Publishers, **2003**. p. 237–265.
5. Guldi D.M. *Chem. Soc. Rev.* **2002**, *31*, 22–36.
6. El-Khouly M.E., Ito O., Smith P.M., D'Souza F. *J. Photochem. Photobiol.* **2004**, *5*, 79–104.
7. Fukuzumi S. *Bull. Chem. Soc. Jpn.* **2006**, *79*, 177–195.
8. Benniston A.C., Harriman A. *Mater. Today* **2008**, *11*, 26–34.
9. Wasielewski M.R. *Acc. Chem. Res.* **2009**, *42*, 1910–1921.
10. Safont-Sempere M.M., Fernāndez G., Würthner F. *Chem. Rev.* **2011**, *111*, 5784–5814.
11. Mironov A.F. *Macroheterocycles* **2011**, *4*, 186–208.
12. Souza F.D., Ito O. *Chem. Soc. Rev.* **2012**, *41*, 86–96.
13. Fukuzumi S., Ohkubo K. *Dalton Trans.* **2013**, *42*, 15846–15858.
14. Rudolf M., Kirner S.V., Guldi D.M. *Chem. Soc. Rev.* **2016**, *45*, 612–630.
15. Karmova F.M., Lebedeva V.S., Mironov A.F. *Russ. J. Gen. Chem.* **2016**, *86*, 2145–2179.
16. KC C.B., D'Souza F. *Coord. Chem. Rev.* **2016**, *322*, 104–141.
17. Llansola-Portoles M.J., Gust D., Moore T.A., Moore A.L. *C.R. Chimie* **2017**, *20*, 296–313.
18. El-Khouly M.E. *J. Photochem. Photobiol. C* **2017**, *31*, 36–83.
19. Sharma S.K., Chiang L.Y., Hamblin M.R. *Nanomedicine* **2011**, *6*, 1813–1825.
20. Paszko E., Ehrhardt C., Senge M.O., Kelleher D.P., Reynolds J.V. *Photodiagn. Photodyn. Ther.* **2011**, *8*, 14–29.
21. Gupta A., Avci P., Sadasivam M., Chandran R., Parizotto N., Vecchio D., de Melo W.C.M.A., Dai T., Chiang L.Y., Hamblin M.R. *Biotechnol. Adv.* **2013**, *31*, 607–631.
22. Lucky S.S., Soo K.C., Zhang Y. *Chem. Rev.* **2015**, *115*, 1990–2042.
23. Nakamura Y., Kato S.-I. *Chem. Rec.* **2011**, *11*, 77–94.
24. Tzirakis M.D., Orfanopoulos M. *Chem. Rev.* **2013**, *113*, 5262–5321.
25. Yamada M., Akasaka T., Nagase S. *Chem. Rev.* **2013**, *113*, 7209–7264.
26. Khakina E.A., Troshin P.A. *Russ. Chem. Rev.* [*Uspekhi Khi-mii,* in Russ.] **2017**, *86*, 805–830.
27. Yurovskay M.A., Trushkov J.V. *Russ. Chem. Bull., Int. Ed.* **2002**, *51*, 367–443.
28. Mateo-Alonso A., Sooambar C., Prato M. *Org. Biomol. Chem.* **2006**, *4*, 1629–1637.
29. Martin N., Altable M., Filippone S., Martin-Domenech A. *Synlett.* **2007**, *18*, 3077–3095.
30. Kharisov B.I., Kharisova O.B., Gomez M.J., Mendez U.O. *Int. Eng. Chem. Res.* **2009**, *48*, 545–571.
31. Hirsch A., Brettreich M. *Fullerenes: Chemistry and Reac-tions*. Wiley-VCH: Weinhem, Germany, **2005**. 445 p.
32. Yang H.-T., Ruan X.-J., Miao C.-B., Sun X.-Q. *Tetrahedron Lett.* **2010**, *51*, 6056–6059.
33. Troshina O.A., Troshin P.A., Peregudov A.S., Kozlovskiy V.I., Balzarini J., Lyubovskaya R.N. *Org. Biomol. Chem.* **2007**, *5*, 2783–2791.
34. Belik A.Yu., Mikhailov P.A., Kraevaya O.A., Rybkin A.Yu., Khakina E.A., Goryachev N.S., Usol'tseva L.I., Romanenko Yu.V., Koifman O.I., Gushchina O.I., Mironov A.F., Troshin P.A., Kotel'nikov A.I. *Dokl. Phys. Chem.* **2017**, *477*, 222–226.
35. Liddell P.A., Sumida J.P., Macpherson A.N., Noss L., Seely G.R., Clark K.N., Moore A.L., Moore T.A., Gust D. *Photo-chem. Photobiol.* **1994**, *60*, 537–541.
36. Bertran J.C., Monforts F.-P. *Eur. J. Org. Chem.* **2017**, 1608–1617.
37. Zheng G., Dougherty T.J., Pandey R.K. *Chem. Commun.* **1999**, 2469–2470.

38. Bourgeois J.P., Diederich F., Echegoyen L., Nierengarten J.-F. *Helv. Chim. Acta* **1998**, *81*, 1835–1844.

39. Armaroli N., Marconi G., Echegoyen L., Bourgeois J.-P., Diederich F. *Chem. Eur. J.* **2000**, *6*, 1629–1645.

40. Bonifazi D., Scholl M., Song F.Y., Echegoyen L., Accorsi G., Armaroli N., Diederich F. *Angew. Chem. Int. Ed.* **2003**, *42*, 4966–4970.

41. Bonifazi D., Accorshi G., Armaroli N., Song F.Y., Palkar A., Echegoyen L., Scholl M., Seiler P., Jaun B., Diederich F. *Helv. Chim. Acta* **2005**, *88*, 1839–1884.

42. Accorshi G., Armoroli N. *J. Phys. Chem. C* **2010**, *114*, 1385–1403.

43. Guldi D.M., Luo C., Prato M., Dietel E., Hirsch A. *Chem. Commun.* **2000**, 373–374.

44. Guldi D.M., Hirsch A., Scheloske M., Dietel E., Troisi A., Zerbetto F., Prato M. *Chem. Eur. J.* **2003**, *9*, 4968–4979.

45. Cheng P., Wilson S.R., Schuster D.I. *Chem. Commun.* **1999**, 89–90.

46. Wedel M., Monforts F.-P. *Tetrahedron Lett.* **1999**, *40*, 7071–7074.

47. Schuster D.I., Cheng P., Wilson S.R., Prokhorenko V., Katterle M., Holzwarth A.R., Braslavsky S.E., Klihm G., Williams R.M., Luo C. *J. Am. Chem. Soc.* **1999**, *121*, 11599–1160.

48. Kovacs C., Hirsch A. *Eur. J. Org. Chem.* **2006**, *2006*, 3348–3357.

49. Spänig F., Kovacs C., Hauke F., Ohkubo K., Fukuzumi S., Gudi D.M., Hirsch A. *J. Am. Chem. Soc.* **2009**, *131*, 8180–8195.

50. Ermilov E.A., Al-Omari S., Helmreich M., Jux N., Hirsch A., Röder B. *Chem. Phys.* **2004**, *301*, 27–31.

51. D'Souza F., Gaddle S., Zandler M.E., Arkady K., El-Khouly M.E., Fujitsuka M. *J. Phys. Chem. A* **2002**, *106*, 12393–12404.

52. El-Khouly M.E., Araki Y., Ito O., Gaddle S., Mc Carty A.L., Karr P.A., Zandler M.E., D'Souza F. *Phys. Chem. Chem. Phys.* **2005**, *7*, 3163–3171.

53. Kashiwagi Y., Ohkubo K., McDonald J.A., Blake I.M., Crossley M.J., Araki Y., Ito O., Imahori H., Fukuzumi S. *Org. Lett.* **2003**, *5*, 2719–2721.

54. Ohkubo K., Kotani H., Shao J., Ou Z., Kadish K.M., Li G., Pandey R.K., Fujitsuka M., Ito O., Imahori H., Fukuzumi S. *Angew. Chem. Int. Ed.* **2004**, *43*, 853–856.

55. Ohkubo K. In: *5th International Conference on Porphyrins and Phthalocyanines (ICPP-5), Book of Abstracts.* Moscow, **2008**. p. 45.

56. Liddell P.A., Kuciauskas D., Sumida J.P., Nash B., Nguen D., Moore A.L., Moore T.A., Gust D. *J. Am. Chem. Soc.* **1997**, *119*, 1400–1405.

57. Luo C., Guldi D.M., Imahori H., Tamaki K., Sakata Y. *J. Am. Chem. Soc.* **2000**, *122*, 6535–6551.

58. Imahori H., Guldi D.M., Tamaki K., Yoshida Y., Luo C., Sakata Y., Fukuzumi S. *J. Am. Chem. Soc.* **2001**, *123*, 6617–6628.

59. Imahori H., Sekiguchi Y., Kashiwagi Y., Sato T., Araki Y., Ito O., Fukuzumi S. *Chem. Eur. J.* **2004**, *10*, 3184–3196.

60. Curiel D., Ohkubo K., Reimers J.R., Fukuzumi S., Crossley M.J. *Phys. Chem. Chem. Phys.* **2007**, *9*, 5260–5266.

61. Crossley M., Govenleek L.J., Prashar J.K. *J. Chem. Soc., Chem. Commun.* **1995**, 2379–2380.

62. Choi M.-S., Aida T., Luo H., Araki Y., Ito O. *Angew. Chem. Int. Ed.* **2003**, *42*, 4060–4063.

63. Kuciauskas D., Liddell P.A., Lin S., Johnson T.E., Weghorn S.J., Lindsey J.S., Gust D. *J. Am. Chem. Soc.* **1999**, *121*, 8604–8614.

64. Herrmann A. Ph.D. Dissertation, University of Erlangen-Nurnberg, **2017**.

65. Kodis G., Liddell P.A., de la Garza, Clausen P.C., Lindsey J.S., Moore A.L., Moore T.A., Gust D. *J. Phys. Chem. A* **2002**, *106*, 2036–2048.

66. El-Khouly M.E., Fukuzumi S., D'Souza F.D. *Chem. Phys. Chem.* **2014**, *15*, 30–47.

67. Liu J.-Y., El-Khouly M.E., Fukuzumi S., Ng D.K.P. *Chem. Eur. J.* **2011**, *17*, 1605–1613.

68. Maggini M., Scorrano G., Prato M. *J. Am. Chem. Soc.* **1993**, *115*, 9798–9799.

69. Wijesinghe C.A., El-Khouly M.E., Zandler M.E., Fukuzumi S., D'Souza F.D. *Chem. Eur. J.* **2013**, *19*, 9629–9638.

70. D'Souza F., Gaddle S., Islam M.S., Wijesinghe C.A., Schumacher A.L., Zandler M.E., Araki Y., Ito O. *J. Phys. Chem. A* **2007**, *111*, 8552–8560.

71. Hizume Y., Tashiro K., Charvet R., Yamamoto Y., Saeki A., Seki S., Aida T. *J. Am. Chem. Soc.* **2010**, *132*, 6628–6629.

72. Charvet R., Yamamoto Y., Sasaki T., Kim J., Kato K., Takata M., Saeki A., Seki S., Aida T. *J. Am. Chem. Soc.* **2012**, *134*, 2524–2527.

73. Milanesio M.E., Alvarez M.G., Rivarola V., Silber J.J., Durantini E.N. *Photochem. Photobiol.* **2005**, *81*, 891–897.

74. Milanesio M.E., Gervaldo M., Otero L.A., Seleno L., Silber J.J., Durantini E.N. *J. Phys. Org. Chem.* **2002**, *15*, 844–851.

75. Lebedeva V.S., unpublished data.

76. Lebedeva V.S., Karmova F.M., Mironov A.F. *Mendeleev Commun.* **2015**, *25*, 32–33.

77. Ballatore M.B., Spesia M.B., Milanesio M.E., Durantini N. *Eur. J. Med. Chem.* **2014**, *83*, 685–694.

78. Lee D.J., Ahn Y.S., Youn Y.S., Lee E.S. *Polym. Adv. Technol.* **2013**, *24*, 220–227.

79. Guan M., Ge J., Wu J., Zhang G., Chen D., Zhang W., Zhang Y., Zon T., Zhen M., Wang C., Chu T., Hao X., Shu C. *Biomaterials* **2016**, *103*, 75–85.